Article

Cell Reports

Mitochondrial Dysfunction Prevents Repolarization of Inflammatory Macrophages

Graphical Abstract

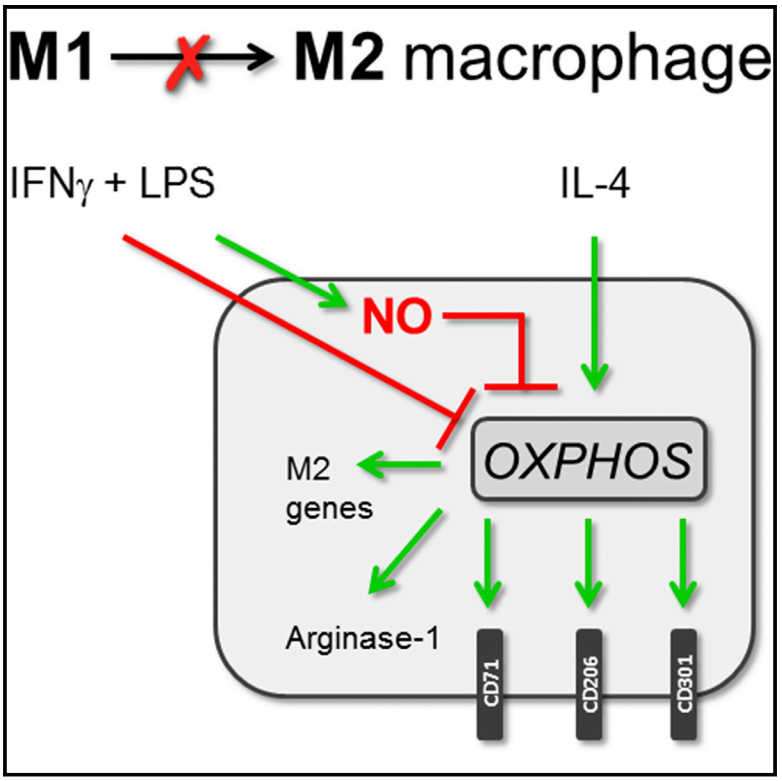

Authors

Jan Van den Bossche, Jeroen Baardman, Natasja A. Otto, ..., Marten A. Hoeksema, Alex F. de Vos, Menno P.J. de Winther

Correspondence

j.vandenbossche@amc.uva.nl

In Brief

Editing macrophage polarization is an emerging concept for the treatment of inflammatory diseases. Van den Bossche et al. show that inflammatory M1 macrophage activation dampens mitochondrial function, thereby preventing the repolarization to an anti-inflammatory M2 phenotype. Inhibiting nitric oxide production improves mitochondrial function and reprogramming to M2 macrophages.

Highlights

- Mouse and human M1 macrophages fail to repolarize to M2 upon IL-4 restimulation
- LPS + IFNγ treatment inhibits mitochondrial oxidative respiration in macrophages
- Mitochondrial function is required for the repolarization to an M2 phenotype
- NO blunts mitochondrial respiration and prevents plasticity in M1 macrophages

Van den Bossche et al., 2016, Cell Reports *17*, 684–696
October 11, 2016
http://dx.doi.org/10.1016/j.celrep.2016.09.008

OPEN ACCESS
CellPress

Cell Reports
Article

Mitochondrial Dysfunction Prevents Repolarization of Inflammatory Macrophages

Jan Van den Bossche,[1,5,*] Jeroen Baardman,[1] Natasja A. Otto,[1,2,3] Saskia van der Velden,[1] Annette E. Neele,[1] Susan M. van den Berg,[1] Rosario Luque-Martin,[1] Hung-Jen Chen,[1] Marieke C.S. Boshuizen,[1] Mohamed Ahmed,[1] Marten A. Hoeksema,[1] Alex F. de Vos,[2,3] and Menno P.J. de Winther[1,4]

[1]Department of Medical Biochemistry, Experimental Vascular Biology, Academic Medical Center, University of Amsterdam, Meibergdreef 9, Amsterdam 1105, the Netherlands

[2]Center for Experimental and Molecular Medicine, Academic Medical Center, University of Amsterdam, Meibergdreef 9, Amsterdam 1105, the Netherlands

[3]Center for Infection and Immunity, Academic Medical Center, University of Amsterdam, Meibergdreef 9, Amsterdam 1105, the Netherlands

[4]Institute for Cardiovascular Prevention (IPEK), Ludwig Maximillian's University, Pettenkoferstrasse 9, Munich 80336, Germany

[5]Lead Contact

*Correspondence: j.vandenbossche@amc.uva.nl

http://dx.doi.org/10.1016/j.celrep.2016.09.008

SUMMARY

Macrophages are innate immune cells that adopt diverse activation states in response to their microenvironment. Editing macrophage activation to dampen inflammatory diseases by promoting the repolarization of inflammatory (M1) macrophages to anti-inflammatory (M2) macrophages is of high interest. Here, we find that mouse and human M1 macrophages fail to convert into M2 cells upon IL-4 exposure in vitro and in vivo. In sharp contrast, M2 macrophages are more plastic and readily repolarized into an inflammatory M1 state. We identify M1-associated inhibition of mitochondrial oxidative phosphorylation as the factor responsible for preventing M1→M2 repolarization. Inhibiting nitric oxide production, a key effector molecule in M1 cells, dampens the decline in mitochondrial function to improve metabolic and phenotypic reprogramming to M2 macrophages. Thus, inflammatory macrophage activation blunts oxidative phosphorylation, thereby preventing repolarization. Therapeutically restoring mitochondrial function might be useful to improve the reprogramming of inflammatory macrophages into anti-inflammatory cells to control disease.

INTRODUCTION

In addition to their function in host defense, macrophages secure tissue homeostasis and dampen inflammatory responses (Okabe and Medzhitov, 2016; Wynn et al., 2013). To carry out these seemingly contrasting functions, macrophages show high plasticity and adopt a spectrum of polarization states, among which M1 and M2 cells are the extremes (Xue et al., 2014). M1 macrophages are induced by the Th1 cytokine interferon-γ (IFNγ) in combination with Toll-like receptor (TLR) ligands, such as lipopolysaccharide (LPS), and they are, therefore, also termed M(LPS + IFNγ) (Murray et al., 2014). These cells secrete pro-inflammatory cytokines; produce reactive oxygen and nitrogen species to ensure efficient microbial killing; and show enhanced MHC-I/II, CD80, and CD86 expression. However, continuous M1 activation may cause collateral tissue damage and chronic inflammation (Sica and Mantovani, 2012).

Macrophages are also activated by diverse non-inflammatory factors. Although non-M1 macrophages are often grouped as M2, the Th2 cytokines IL-4 and IL-13 are the only inducers of the so-called alternatively activated macrophages (AAMs; M[IL-4] and M2a) (Gordon and Martinez, 2010; Murray et al., 2014; Sica and Mantovani, 2012). Functionally, M2 macrophages dampen Th1/M1-driven inflammation, promote tissue repair, and mediate Th2-driven pathologies, such as asthma and helminth infections. At the molecular level, M2 macrophages are characterized by a range of specific marker genes, surface markers, and enzymes (Gordon and Martinez, 2010; Martinez et al., 2013; Van den Bossche et al., 2009, 2012). For clarity, we will hereafter refer to IL-4-induced macrophages as M2 and to LPS + IFNγ-elicited macrophages as M1 cells.

Editing macrophage (re)polarization is emerging as a new therapeutic approach (Hagemann et al., 2008; Sica and Mantovani, 2012; Wynn et al., 2013). For example, reprogramming tumor-promoting M2-like tumor-associated macrophages into anti-tumor M1-like cells is being tested as a cancer treatment (Colombo et al., 1992; Hagemann et al., 2008; Sica and Mantovani, 2012). Conversely, the treatment of chronic inflammatory diseases, such as atherosclerosis and rheumatoid arthritis, will benefit from the repolarization of inflammatory M1 into anti-inflammatory M2 macrophages. While the apparent switch from M1 to M2 characterizes the course of repair and anti-microbial responses (Das et al., 2015; Rigamonti et al., 2014; Van den Bossche et al., 2009; Wynn et al., 2013), in vivo evidence of M1→M2 repolarization is lacking. Indeed, it is a continuing debate whether the sequential presence of M1 and M2 macrophages

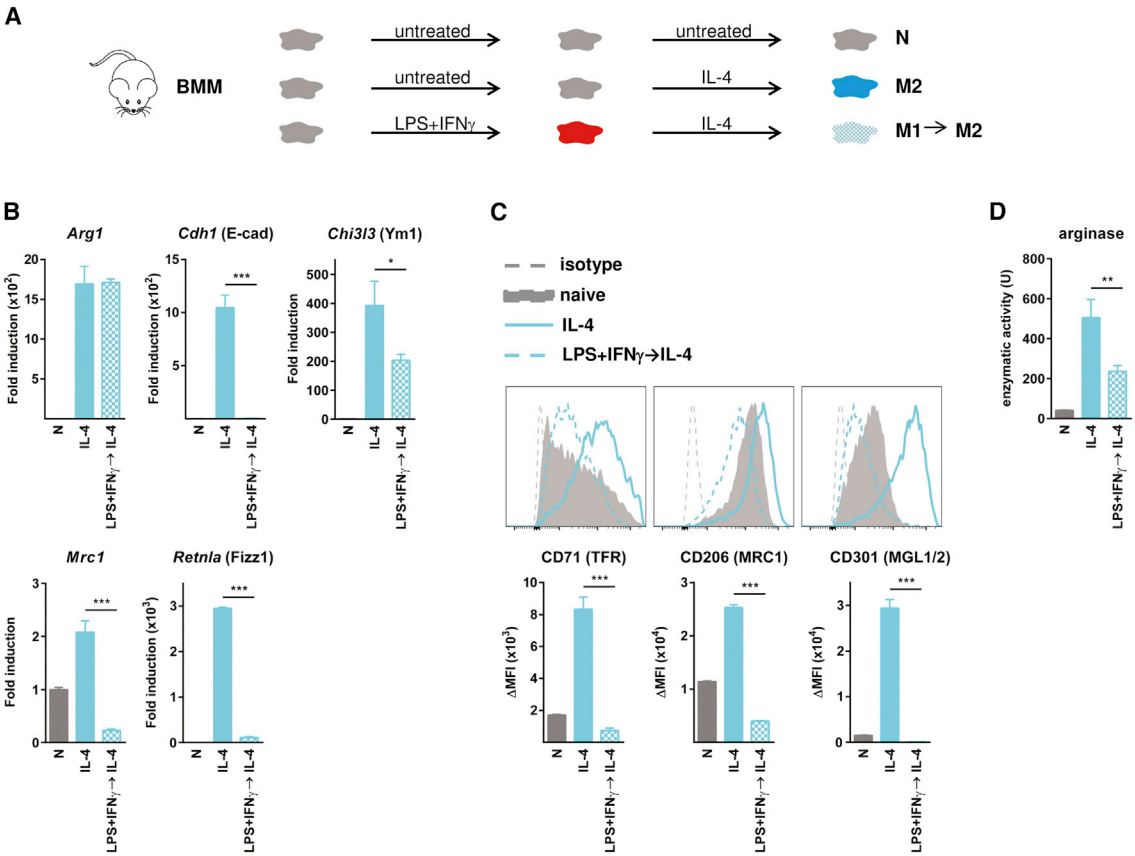

Figure 1. LPS + IFNγ-Primed Mouse M1 Macrophages Fail to Repolarize to M2 Cells upon IL-4 Restimulation

(A) To study the repolarization capacity of mouse bone marrow-derived macrophages (BMMs), normal M2 macrophages were compared to M1→M2 macrophages that were primed for 24 hr with LPS + IFNγ before 24 hr IL-4 stimulation.

(B) The fold inductions of indicated IL-4-induced M2 marker genes are shown relative to the expression in untreated macrophages (= 1).

(C) Differentially treated macrophages were stained with antibodies against the M2 surface markers CD71 (TFR, transferrin receptor), CD206 (MRC1, mannose receptor C type 1), CD301 (MGL1/2, macrophage galactose-binding lectin), or isotype control, followed by flow cytometric analysis. Representative histogram graphs and corresponding surface expression quantifications (ΔMFI = [Median fluorescence intensity]$_{\text{positive staining}}$ – [Median fluorescence intensity]$_{\text{isotype staining}}$) are presented.

(D) Arginase activity in BMM lysates was measured and shown as units (U) enzymatic activity. Values represent mean ± SEM of three mice (*$p < 0.05$, **$p < 0.01$, and ***$p < 0.001$; ns, not significant).

results from actual repolarization as a response to the changing microenvironment or from the recruitment of new monocytes to a repair-promoting local milieu (Das et al., 2015; Italiani and Boraschi, 2014; Rigamonti et al., 2014).

Metabolic cascades are increasingly recognized as characteristics and controllers of macrophage activation (Galván-Peña and O'Neill, 2014; Jha et al., 2015; Ouimet et al., 2015). M1 cells use glycolysis for rapid killing, whereas M2 macrophages rely on mitochondrial oxidative phosphorylation (OXPHOS) for sustained energy production (Cramer et al., 2003; Huang et al., 2014; Tan et al., 2015; Tannahill et al., 2013; Vats et al., 2006). These metabolic cascades do not only reflect macrophage energy production but also directly dictate the phenotype. As such, glycolysis drives inflammatory macrophage responses (Cramer et al., 2003; Tannahill et al., 2013), and OXPHOS supports M2 activation (Tan et al., 2015; Vats et al., 2006).

Here, we show that M1 activation inhibits mitochondrial function, thereby impairing future IL-4-responses. Inhibiting inducible nitric oxide synthase (iNOS) in mouse macrophages dampened the LPS + IFNγ-induced decline in mitochondrial respiration and improved the metabolic and phenotypic M1→M2 repolarization.

RESULTS

Mouse M1 Macrophages Fail to Repolarize to M2 upon IL-4 Restimulation In Vitro

Given that the treatment of chronic inflammatory diseases could profit from the repolarization of inflammatory into anti-inflammatory macrophages, we assessed the repolarization capacity of M1 cells. Hereto, we first compared the IL-4-induced response of mouse bone marrow-derived macrophages (BMMs) that had been pre-treated with LPS + IFNγ (Figure 1A, cyan checkered) with the response of normal M2 cells (cyan). Inflammatory M1 macrophages did not exhibit efficient upregulation of the M2-specific marker genes *Cdh1* (E-cad), *Chi3l3*, *Mrc1*, and

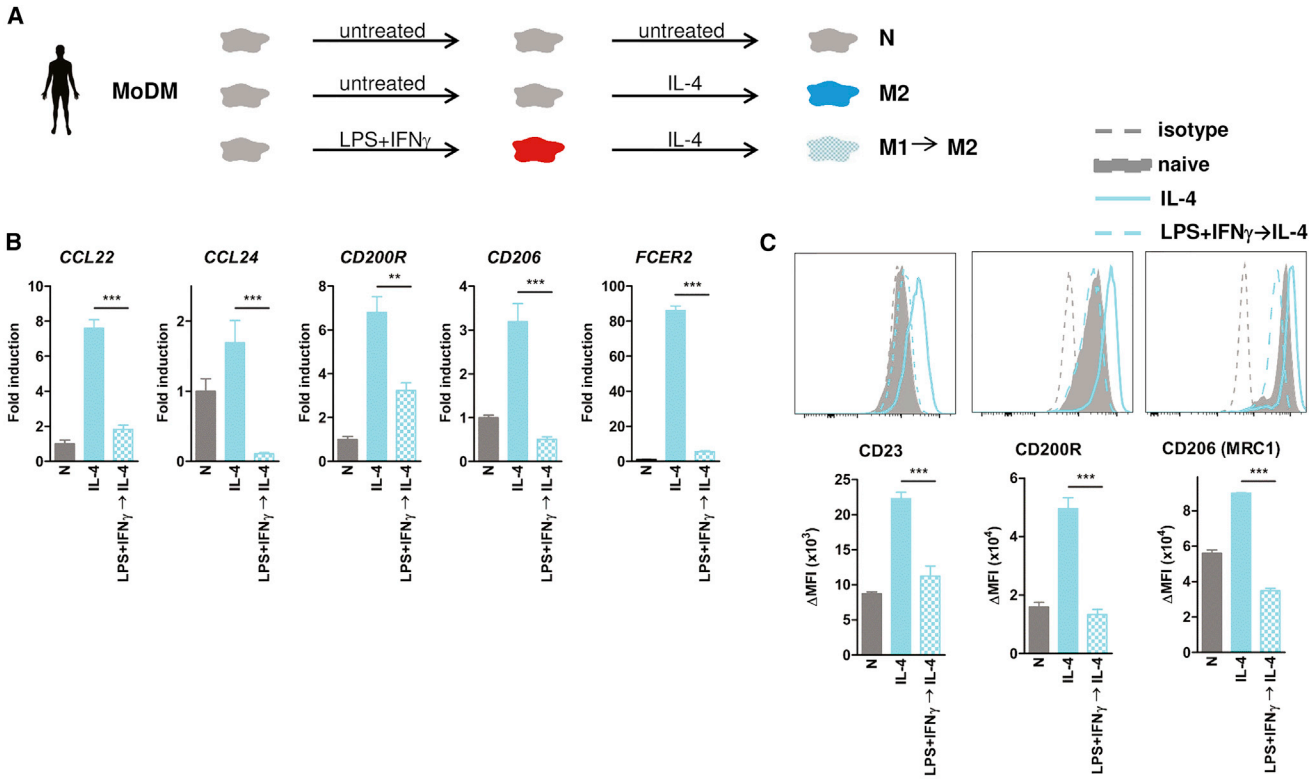

Figure 2. Human Macrophages Show No M1→M2 Repolarization

(A) To study the plasticity of human M1 macrophages, peripheral blood monocyte-derived macrophages (MoDMs) were primed with LPS + IFNγ or left untreated. After 24 hr, cells were washed and treated with IL-4 for another 24 hr, or they remained untreated as a control. IL-4-induced M2 macrophages were compared to M1→M2 macrophages that were primed with LPS + IFNγ before IL-4 treatment.

(B) The fold inductions of the indicated M2-associated genes are shown relative to the expression in untreated macrophages (= 1).

(C) (Re)polarized macrophages were stained with antibodies against CD14, CD23, CD200R, CD206, or isotype controls, followed by flow cytometric analysis. Representative histogram overlays for differentially treated $CD14^+$ macrophages, together with the quantified surface expression values (ΔMFI = [Median fluorescence intensity]$_{\text{positive staining}}$ – [Median fluorescence intensity]$_{\text{isotype staining}}$) are shown. Values represent mean ± SEM of three wells of one representative donor (of three tested donors) (*$p < 0.05$, **$p < 0.01$, and ***$p < 0.001$; ns, not significant).

Retnla, when the cells were washed and stimulated 30 min afterward with IL-4 for 24 hr (Figure 1B). Also, when the M1 cells were allowed to recover for 24 hr between the first inflammatory response and the subsequent M2 repolarization, IL-4 failed to elicit an efficient M2 gene signature (Figure S1). In accordance with the gene expression data, the M2 surface markers CD71, CD206, and CD301 were not induced by IL-4 following LPS + IFNγ stimulation (Figure 1C). Despite the fact that *Arg1* gene expression was plastic and was still inducible by IL-4 after LPS + IFNγ stimulation (Figure 1B), M1→M2 macrophages showed significantly less IL-4-induced arginase function compared to M2 cells (Figure 1D). Likewise, LPS + IFNγ pretreatment impaired the induction of an IL-10-elicited M2-like phenotype (Figure S2).

Next, we studied the capacity of M2 macrophages to mount an inflammatory response by comparing the LPS + IFNγ-induced response of M2→M1 (Figure S3A, red checkered) with the response of normal M1 cells (red). We found that, independent of the first stimulus, LPS + IFNγ efficiently induced the M1-associated genes *Il12b*, *Il1b*, *Il6*, *Nos2*, and *Tnf* in both M2→M1 and M1 cells (Figure S3B). The repolarization capacity of IL-4-induced macrophages was further reflected at the protein level, as M2→M1 and M1 macrophages displayed identical CD80 and CD86 expression (Figure S3C) Functionally, M2→M1 and M1 macrophages showed similar inflammatory cytokine secretion and iNOS-mediated nitric oxide (NO) production (Figures S3D and S3E). Thus, while mouse M2 macrophages readily repolarized to a pro-inflammatory state upon LPS + IFNγ restimulation, M1 activation prevented subsequent M2 polarization in vitro.

Human Inflammatory Macrophages Do Not Repolarize to M2

To test the relevance of these findings for humans, we studied the M1→M2 repolarization of peripheral blood monocyte-derived human macrophages (MoDMs) (Figure 2A). Confirming our studies with mouse macrophages, human M1 macrophages showed strongly impaired IL-4-induced expression of the M2 marker genes *CCL22*, *CCL24*, *CD200R*, *CD206*, and *FCER2* (CD23) (Figure 2B). In accordance, the M2 surface markers CD23, CD200R, and CD206 were not induced by IL-4 after prior LPS + IFNγ stimulation (Figure 2C).

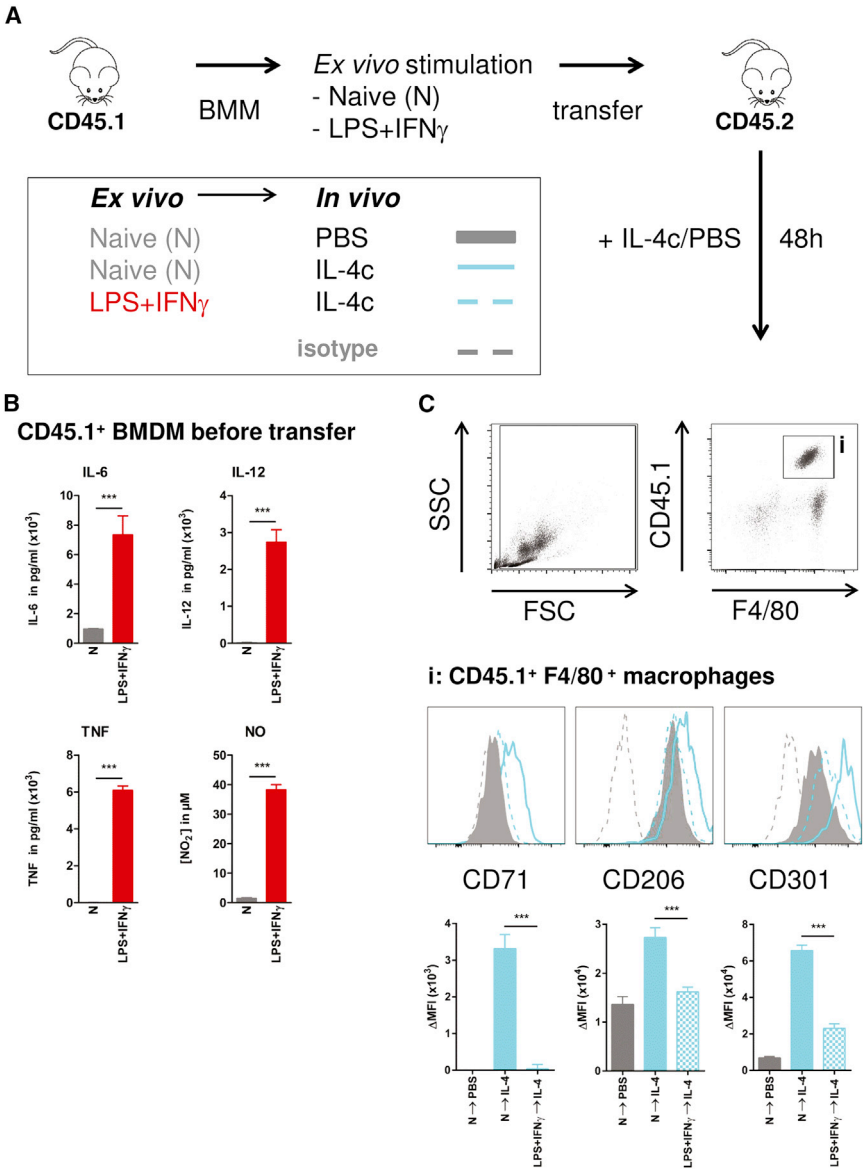

Figure 3. Ex-Vivo-Stimulated M1 Macrophages Do Not Repolarize to M2 In Vivo in Response to an IL-4 Challenge

(A) To assess in vivo M1→M2 repolarization after IL-4 injection, BMMs from CD45.1 donor mice were stimulated with LPS + IFNγ (red) or left untreated (gray).

(B) After 24 hr, these CD45.1$^+$ macrophages were assessed for efficient M1 polarization, and they were transferred to CD45.2 acceptor mice that next received IL-4c (or PBS as a control).

(C) After 48 hr, flow cytometry was performed on the peritoneal cells to assess CD71, CD206, and CD301 M2 surface marker expression on CD45.1$^+$ F4/80$^+$ adoptively transferred macrophages (gate i). As such, M2 polarization (cyan bars) and M1→M2 repolarization (cyan checkered bars) were measured and presented as ΔMFI = (Median fluorescence intensity)$_{\text{positive staining}}$ − (Median fluorescence intensity)$_{\text{isotype staining}}$. Values represent mean ± SEM of four mice (*p < 0.05, **p < 0.01, and ***p < 0.001).

Thus, both mouse and human macrophages completely failed to accept an IL-4-induced state after a preceding inflammatory stimulus.

Conversely, human IL-4-induced M2 cells reversed to an inflammatory state upon LPS + IFNγ treatment, as evidenced by the high expression of M1 marker genes and surface markers and by the enhanced secretion of inflammatory cytokines (Figures S4A–S4D). Thus, while M2→M1 repolarization efficiently occurred in both mouse and human macrophages, the opposite M1→M2 conversion was impossible.

Inflammatory Macrophages Fail to Repolarize to M2 In Vivo

Next, we studied whether the M1→M2 repolarization defect that we observed in vitro also has relevance in vivo. To test this, untreated (N) or LPS + IFNγ-treated (M1) BMMs from CD45.1$^+$ donor mice were adoptively transferred intraperitoneally to CD45.2$^+$ acceptor mice, which next received an intraperitoneal challenge with IL-4c to induce M2 polarization (Figure 3A). LPS + IFNγ-treated macrophages showed strongly enhanced inflammatory cytokine secretion and NO production (Figure 3B). Confirming our mouse and human in vitro observations, these M1-primed macrophages failed to upregulate CD71, CD206, and CD301 M2 surface marker expression upon in vivo IL-4 challenge (Figure 3C, cyan checkered boxes). Demonstrating the efficiency of this in vivo challenge protocol, adoptively transferred naive CD45.1$^+$ macrophages (Figure 3C, cyan) and CD45.2$^+$-resident macrophages (data not shown) efficiently upregulated the tested M2 surface markers upon IL-4c administration.

Overall, we showed that M1 macrophages also failed to convert into M2 cells upon an IL-4 challenge in vivo.

LPS + IFNγ Treatment Blunts Mitochondrial Oxidative Respiration in Mouse Macrophages

Next, we further studied mouse BMMs to identify why M1 cells are unable to repolarize to M2. Because the minimum requirement for M1→M2 repolarization is an intact IL-4Rα-JAK-STAT6 pathway, we first assessed IL-4Rα expression and STAT6 phosphorylation. IL-4Rα levels were compared among naive, LPS + IFNγ-induced M1, IL-4-induced M2, and M1→M2 macrophages (Figure 4A). M1 polarization actually enhanced IL-4Rα levels and also M1→M2 repolarized macrophages had increased levels compared to M2. Accordingly,

M1→M2 repolarized macrophages showed effective STAT6 phosphorylation (Figure 4B). When assessing the viability of differentially stimulated macrophages, we observed a similar percentage of annexin V^- propidium iodide $(PI)^-$ living cells under all tested conditions (Figure 4C). However, M1 macrophages were less active than naive and, especially, M2 cells in the 3-(4,5-dimethylthiazol-2-yl)-2,5-diphenyl tetrazolium bromide (MTT) assay (Figure 4D).

Although this assay is often used to assess cell viability, it actually measures succinate dehydrogenase activity and, thus, mitochondrial function. Given identical annexin V PI staining (Figure 4), the changes observed in the MTT assay suggest metabolic differences in these macrophages. This prompted us to assess the metabolic characteristics of (re)polarized macrophages by extracellular flux analysis, particularly because recent evidence shows that macrophage polarization requires metabolic reprogramming (Galván-Peña and O'Neill, 2014). Changes in extracellular acidification rate (ECAR) in response to glucose, oligomycin (OM), and 2-deoxyglucose (2-DG) injection were used to calculate all glycolysis parameters. In parallel, OXPHOS characteristics were calculated from the changes in oxygen consumption rate (OCR) in response to OM, carbonyl cyanide 4-(trifluoromethoxy)phenylhydrazone (FCCP), and rotenone (ROT) + antimycin A (AA) injection, as detailed in Figure S5. We confirmed that M2 macrophages show enhanced OXPHOS and have the capacity to switch to glycolysis when mitochondrial ATP production is blocked with OM (Figures 4E–4G). In contrast, M1 macrophages exhibited increased glycolysis, complete suppression of OXPHOS, and reduced fatty acid oxidation (FAO) (Figures 4E–4H).

To gain insight into the mechanism of reduced mitochondrial oxygen consumption in M1 macrophages, we examined the effect of LPS + IFNγ on different established metabolic readouts. Mitochondrial dysfunction in M1 cells was not caused by an LPS + IFNγ-mediated suppression of mitochondrial (and glycolysis) genes nor by a reduction of mitochondrial mass, as demonstrated alike by MitoTracker Green staining and mtDNA/genomic DNA (gDNA) ratio (Figures S6A–S6D). Also, the activity of citrate synthase, the pacemaker enzyme of the Krebs cycle, was not impaired in M1 (Figure S6E). Next, we measured the activity of the individual mitochondrial respiratory complexes I–IV (calculated as described in Table S1), using an established extracellular flux analysis protocol. LPS + IFNγ treatment completely suppressed complex I and II activity and dampened complex II and IV activity partially (Figure 4I, red bars). Importantly, the LPS + IFNγ-mediated inhibition of the distinct electron transport chain complexes could not be restored by subsequent IL-4 restimulation (blue/white bars). Also, in intact cells, the LPS + IFNγ-mediated suppression of mitochondrial respiration was not restored after subsequent IL-4 treatment, as demonstrated by the highly suppressed basal respiration, ATP synthase activity, maximal respiration, and spare respiratory capacity (calculated as described in Figure S5) observed in M1→M2 cells compared with naive controls and normal M2 macrophages (Figure 4J). Thus, M1 macrophages failed to repolarize to M2 cells phenotypically, functionally, and metabolically.

Mitochondrial Function Is Required for the Induction of an M2 Phenotype

Given that increased mitochondrial metabolism is both a characteristic of and requirement for the anti-inflammatory responses of M2 macrophages (Huang et al., 2014; Tan et al., 2015; Vats et al., 2006), the suppression of OXPHOS by LPS + IFNγ may impede M1→M2 repolarization. In support of this hypothesis, blocking mitochondrial ATP synthase activity with OM before IL-4 stimulation dampened OCRs (Figure 5A) and, thereby, completely abolished IL-4-induced *Arg1*, *Cdh1*, *Chi3l3*, and *Retnla* expression (Figure 5B). In the absence of mitochondrial ATP production, these macrophages relied on increased glycolysis to fulfill their energy demands (Figure 5A). Depending on the situation, both glucose and FAO can fuel mitochondrial function in M2 macrophages (Huang et al., 2014; Namgaladze and Brüne, 2014; Tan et al., 2015; Vats et al., 2006). In the settings tested in the present study, 2-DG-mediated blocking of the glycolytic flux suppressed mitochondrial respiration (Figure 5A) and impaired M2-associated gene expression (Figure 5B). While FAO was suppressed by LPS + IFNγ stimulation (Figure 4H), inhibiting FAO with etomoxir (ETO) did not prevent the induction of most M2-associated genes (Figure 5B). Confirming our gene expression data, macrophages pre-treated with 2-DG and, especially, OM exhibited a reduction of IL-4-induced CD71, CD206, and CD301 expression and arginase-1 activity (Figures 5C and 5D). Overall, these experiments showed that LPS + IFNγ inhibited glucose-fueled mitochondrial respiration, thereby trapping macrophages in a metabolic state that prevented future IL-4-induced polarization.

NO Blunts Mitochondrial Respiration and Prevents Plasticity in M1 Macrophages

Next, we aimed to identify the mechanism underlying the LPS + IFNγ-induced decline in mitochondrial function and prevention of future IL-4 responses. M1 cells display various features that could impede mitochondrial function and M1→M2 repolarization. First, if the macrophage metabolic machinery itself lacks plasticity, the induction of glycolysis by LPS + IFNγ might impair subsequent IL-4-induced reprogramming toward OXHPOS. Moreover, as an antimicrobial mechanism, M1 cells produce reactive oxygen species (ROS) and iNOS-generated NO, which both inhibit mitochondrial function in other cell types (Everts et al., 2012; Raza et al., 2014).

To assess these alternatives, we pre-treated macrophages with the glycolysis inhibitor 2-DG, the ROS scavenger N-acetylcysteine (NAC), or the iNOS inhibitor 1400W (Garvey et al., 1997), followed by LPS + IFNγ treatment (Figures 6A–6D). Only iNOS inhibition markedly improved mitochondrial function in M1 macrophages, as demonstrated by a pronounced increase in basal respiration, mitochondrial ATP production, and maximal respiration in 1400W-pre-treated M1 cells (Figure 6E). While scavenging ROS with NAC did not improve mitochondrial function, 2-DG-treated M1 macrophages showed a slight increase in mitochondrial ATP production, possibly caused by the 2-DG-mediated inhibition of LPS + IFNγ-induced NO production (Figures 6D and 6E).

Because iNOS inhibition dampened the LPS + IFNγ-induced decline in mitochondrial function, we next tested whether this

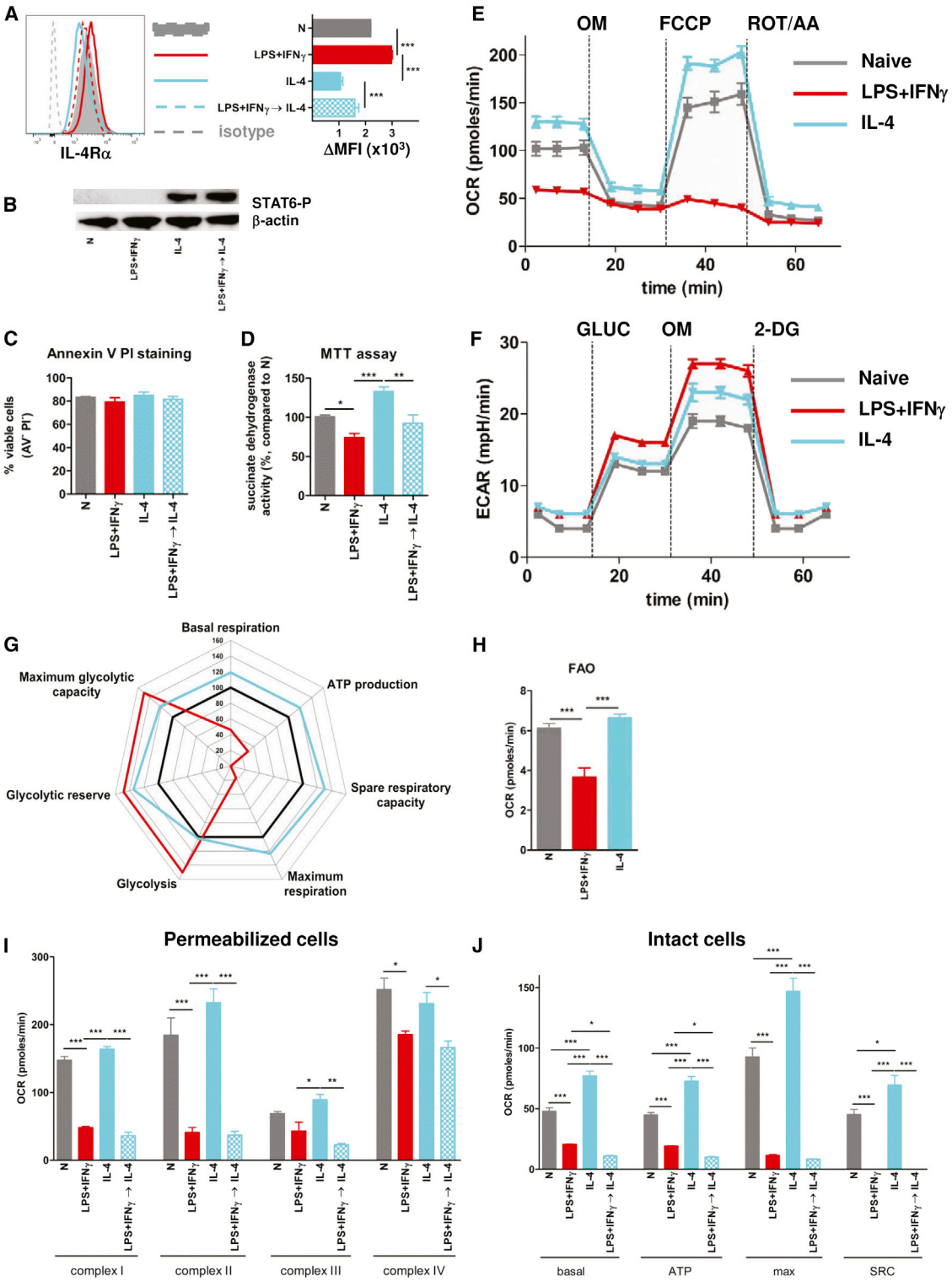

Figure 4. LPS + IFNγ Treatment Impairs OXPHOS and This Effect Cannot Be Reserved by IL-4 upon Repolarization

To study why M1 macrophages do not repolarize to M2 cells, we first assessed IL-4Rα/STAT6 signaling and cell viability in M1, M2, and M1→M2 macrophages.

(A) A representative IL-4α histogram and corresponding quantifications (ΔMFI = [Median fluorescence intensity]$_{\text{positive staining}}$ − [Median fluorescence intensity]$_{\text{isotype staining}}$) are depicted.

(B) Cell lysates were immunoblotted with antibodies against p-STAT6 or actin.

(legend continued on next page)

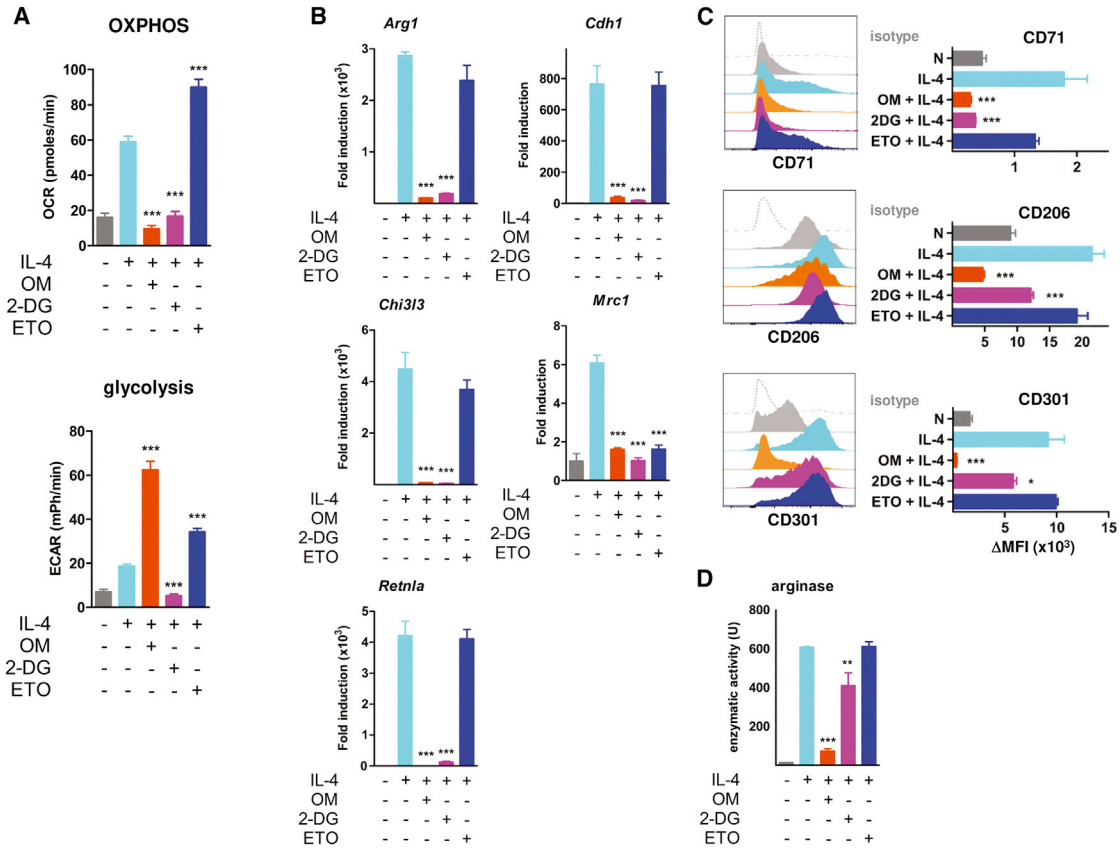

Figure 5. M2 (Re)polarization Needs Glucose-Fueled OXPHOS

For all assays, BMMs were pre-treated with OM, 2-DG, or etomoxir (ETO) or left untreated, followed by IL-4 stimulation in the presence of the inhibitors.

(A) Basal OCR and ECAR rates were measured by extracellular flux analysis as a measurement for OXPHOS and glycolysis, respectively.

(B) The gene expression levels of indicated IL-4-induced M2 marker genes are shown relative to the expression in untreated macrophages (= 1).

(C) BMMs were stained with antibodies against the M2 surface markers CD71 (TFR), CD206 (MRC1), CD301 (MGL1/2), or isotype control, followed by flow cytometric analysis. Representative histogram plots, together with the quantified surface expression values (ΔMFI = [Median fluorescence intensity]$_{\text{positive staining}}$ − [Median fluorescence intensity]$_{\text{isotype staining}}$), are shown.

(D) Arginase activity in BMM lysates was calculated and plotted as units (U) enzymatic activity. Values represent mean ± SEM of three mice (*$p < 0.05$, **$p < 0.01$, and ***$p < 0.001$; ns, not significant).

strategy also could promote future IL-4 responses. For this purpose, we performed repolarization experiments in the presence of the iNOS inhibitor 1400W. iNOS inhibition during the first LPS + IFNγ response markedly improved subsequent IL-4-induced metabolic reprogramming toward enhanced OXPHOS. Indeed, 1400W-pre-treated M1→M2 macrophages showed significantly higher basal respiration, ATP production, and maximal respiration compared with M1→M2 macrophages in which iNOS was not inhibited (Figure 6F). Accordingly, iNOS inhibition improved the activity of complexes I–IV of the electron transport chain in M1→M2 repolarized macrophages, as demonstrated by extracellular flux analysis on permeabilized macrophages and by the MTT assay (Figures 6G and 6H).

(C) BMMs were subjected to Annexin V plus PI staining to determine the percentage of AV^{-} PI^{-} viable cells.

(D) MTT assay was performed to measure mitochondrial succinate dehydrogenase activity.

(E–G) BMMs were seeded in Seahorse plates and stimulated for 24 hr. During extracellular flux analysis, cells were sequentially treated with (E) glucose, oligomycin (OM), and 2-deoxyglucose (2-DG), to determine glycolysis parameters from the ECAR levels, or with (F) OM, FCCP, and rotenone (ROT) plus antimycin A (AA), to assess OXPHOS parameters from the OCR levels. (G) All calculated metabolic parameters in M1 and M2 cells are shown relative to those in naive macrophages (N = 100%).

(H) Fatty acid oxidation (FAO) rates in naive, M1, and M2 macrophages were measured as described previously (Zhang et al., 2012). To compare mitochondrial function in polarized and repolarized macrophages, BMMs were treated as indicated, followed by OCR measurement.

(I) Plasma membrane-permeabilized macrophages were provide with a cocktail of specific substrates and inhibitors to measure complex I-, II-, III-, and IV-mediated respiratory activity. Data were plotted as OCR in pmoles/min.

(J) Using intact cells, the basal respiration, mitochondrial ATP production, maximal respiration, and spare respiratory capacity (SRC) were calculated and plotted as OCR in pmoles/min. Values represent mean ± SEM of three mice (*$p < 0.05$, **$p < 0.01$, and ***$p < 0.001$; ns, not significant).

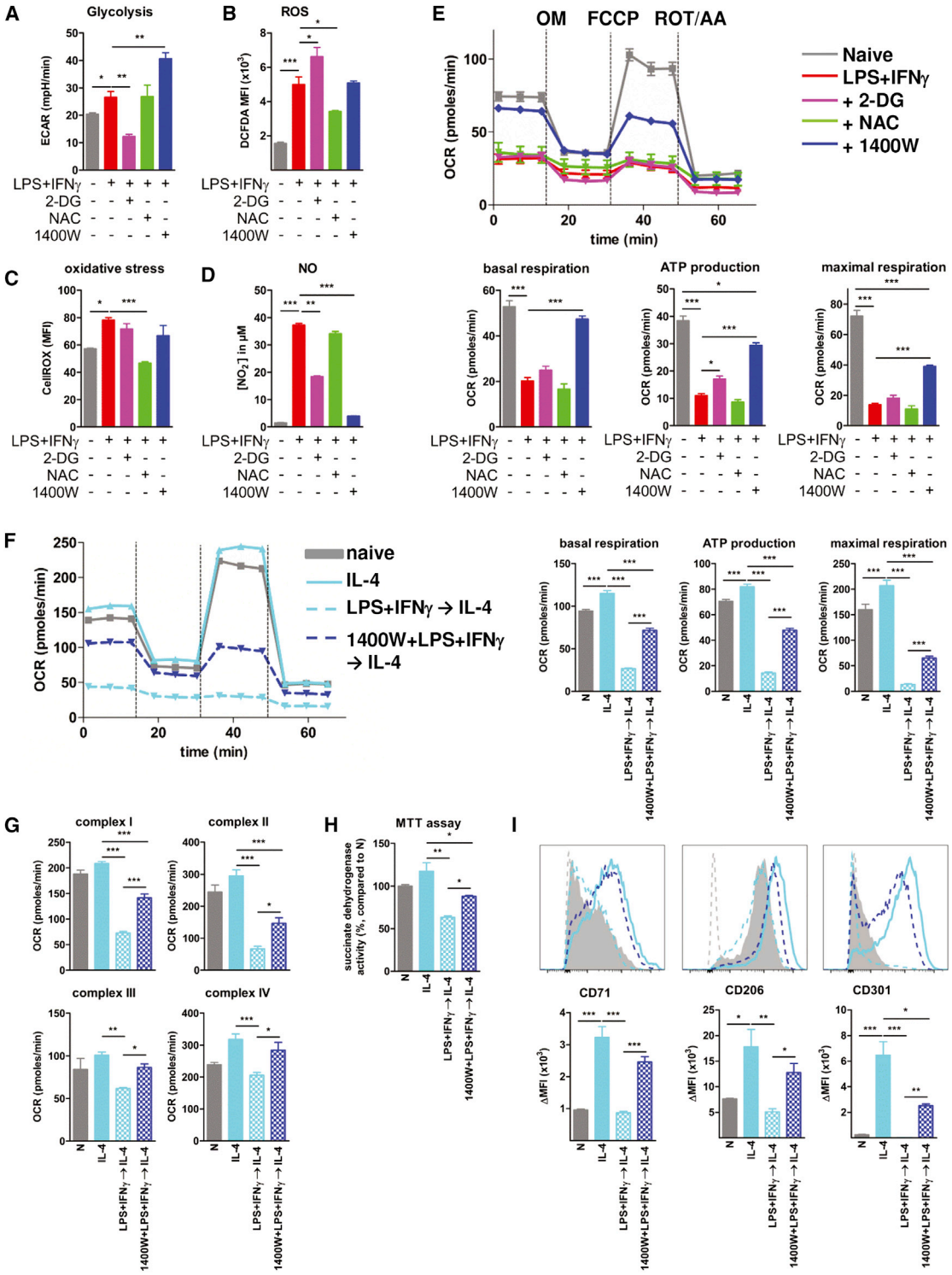

Figure 6. iNOS Inhibition Improves OXPHOS and M1 to M2 Repolarization

(A–D) Macrophages were pre-treated with glycolysis inhibitor 2-DG, ROS scavenger NAC, or iNOS inhibitor 1400W, followed LPS + IFNγ treatment in the presence of the compounds. To demonstrate the respective efficacy of the distinct compounds, we measured (A) glycolysis as extracellular acidification (ECAR), (B) ROS with DCFDA, (C) oxidative stress with CellROX, and (D) NO production.

(E) OXPHOS parameters were assessed by recording the OCR values after sequential injection of OM, FCCP, and ROT + AA. Calculated basal respiration, ATP production, and maximal respiration were plotted in bar graphs.

(legend continued on next page)

Importantly, the repair of mitochondrial function via iNOS inhibition was sufficient to significantly improve the repolarization capacity of M1 cells. As such, iNOS inhibition during the first M1 polarization improved the phenotypic plasticity of the cells, as demonstrated by the enhancement of IL-4-induced CD71, CD206, and CD301 expression in these macrophages (Figure 6I).

iNOS inhibition had no effect on M2 polarization, as pre-treatment with 1400W did not affect the IL-4-induced expression of M2-associated genes and surface markers (Figure S7A). Moreover, the enhanced plasticity of 1400W-pre-treated M1 macrophages was effectively due to the iNOS inhibitory effect of 1400W and not to overall inhibition of the first LPS + IFNγ response. Indeed, 1400W did not block MHC-II, CD80, and CD86 expression (Figure S7B) or inflammatory cytokine secretion (Figure S7C). Thus, iNOS inhibition did not affect M1 and M2 polarization per se but improved M1 → M2 repolarization.

Confirming these assays, *Nos2*$^{-/-}$ macrophages showed improved M1 → M2 phenotypic repolarization, associated with improved mitochondrial respiration. Evidently, *Nos2*$^{-/-}$ macrophages did not produce NO, but exhibited normal M1 and M2 polarization (Figures S8A–S8F) Thus, NO impeded M1 → M2 repolarization, but did not affect M1 and M2 polarization as such.

DISCUSSION

Distinct arginine metabolism was one of the first characteristics employed to define macrophage subsets (Munder et al., 1998). M1 cells convert arginine into NO through iNOS activity and are crucial for host defense. However, sustained M1 activation can cause tissue damage and chronic inflammation. Therefore, a repair phase has to be initiated in which M2 cells predominate. As the yin to the yang of M1, M2 macrophages are low in iNOS, show high arginase-1 activity, and promote tissue repair and resolution of inflammation (Van den Bossche et al., 2012). As such, the course of infections and healing responses is often characterized by an apparent switch from M1 to M2 polarization (Das et al., 2015; Rigamonti et al., 2014; Van den Bossche et al., 2009). This transition can be caused by actual reprogramming of macrophages and/or replacement of M1 cells with recruited monocytes that differentiate into M2 under the influence of the newly established environment (Das et al., 2015). Reshaping unbalanced macrophage polarization has been suggested as the holy grail of macrophage therapeutic targeting (Sica and Mantovani, 2012). In support of this notion, reversal of M2-like tumor-associated macrophages into tumor-killing phagocytes has been used with great success in cancer therapy (Allavena et al., 1990; Colombo et al., 1992; Hagemann et al., 2008).

We now show that M2 macrophages are indeed highly plastic and easily adopt an M1-like inflammatory state. In sharp contrast, M1 cells completely fail to repolarize to M2 in vitro and in vivo, as demonstrated by strongly reduced M2-associated gene and surface protein expression. In support of our findings, previous studies have shown that in vitro IFNγ priming dampens successive IL-4-induced expression of multiple M2-associated genes (Davis et al., 2013; Khallou-Laschet et al., 2010). Furthermore, from a functional perspective, M1 → M2 repolarized macrophages showed aberrant arginase activity and strongly impaired OXPHOS. Importantly, our thorough phenotypic, functional, and metabolic characterization supports our findings of irreversibility of M1 → M2 polarization. If only the *Nos2*/*Arg1* balance were employed as a readout for M1/M2, we would have incorrectly concluded that both M1 and M2 macrophages are fully reversible. Indeed, confirming previous data (Davis et al., 2013), Arg1 was the only M2-associated gene that was still fully induced by IL-4 after prior LPS + IFNγ treatment. Otherwise, M1 cells completely failed to repolarize to M2 macrophages.

We found that the metabolic characteristics of M1 cells prevented repolarization to an M2 state. Inhibiting OXPHOS through LPS + IFNγ stimulation or via OM-mediated inhibition of ATP synthesis completely abolished M2 (re)polarization. Mitochondrial respiration was mainly fueled by glycolysis and not by FAO. These data contribute to the current opinion that the effect of ETO on M2 polarization is more complicated than previously envisioned (Huang et al., 2014; Namgaladze and Brüne, 2014; Tan et al., 2015; Vats et al., 2006). Confirming our observations, a very recent study applied a genetic strategy to disrupt FAO in macrophages and showed no role for FAO in M2 polarization (Nomura et al., 2016).

Our data support the idea that inflammatory triggers induce glycolysis to rapidly provide energy for the clearance of intracellular pathogens by ROS and NO. We now show that, as a consequence of this respiratory burst, LPS + IFNγ induces mitochondrial dysfunction that cannot be restored by subsequent IL-4 stimulation, thereby directly hampering M1 → M2 repolarization. Inhibiting LPS + IFNγ-induced NO production reduced mitochondrial dysfunction and improved phenotypic and metabolic M1 → M2 repolarization. NO and NO-derived reactive nitrogen species can inactivate all iron-sulfur-containing complexes of the mitochondrial electron transport chain (Brown and Borutaite, 2007; Chénais et al., 2002; Pearce and Pearce, 2013). We found LPS + IFNγ to decrease mainly complex I and complex II activity, with minor effects on complexes III and IV. This decline could not be reversed by IL-4, but it was at least partially prevented by iNOS inhibition.

To overcome mitochondrial dysfunction, glycolysis is necessary to maintain ATP production in NO-producing dendritic cells (Everts et al., 2012). It has been suggested that increased

(F) Similarly, OXPHOS in M1 → M2 repolarized macrophages (pre-treated or not with the iNOS inhibitor 1400W) was assessed and compared to the OCR values in normal M2 cells.

(G) Complex I-, II-, III-, and IV-mediated OCR values were measured in plasma membrane-permeabilized macrophages and plotted in pmoles/min.

(H) Mitochondrial succinate dehydrogenase activity in differentially treated macrophages was measured using an MTT assay.

(I) The phenotypic M1 → M2 repolarization of normal M1 cells and M1 macrophages with inhibited iNOS was assessed by flow cytometry for M2 markers CD71, CD206, and CD301 in comparison to the levels in normal M2 macrophages. Representative histograms, together with the quantified expression values (ΔMFI = $[\text{Median fluorescence intensity}]_{\text{positive staining}} - [\text{Median fluorescence intensity}]_{\text{isotype staining}}$), are shown. Values represent mean ± SEM of three mice (*$p < 0.05$, **$p < 0.01$, and ***$p < 0.001$; ns, not significant).

glycolysis in inflammatory macrophages is mainly caused by reactive nitrogen species (Albina and Mastrofrancesco, 1993). However, our data demonstrate that the enhanced glycolysis observed in M1 cells is not simply a consequence of NO production and associated mitochondrial dysfunction. In fact, LPS + IFNγ treatment in the presence of the iNOS inhibitor induces even higher glycolysis, emphasizing that additional factors, such as HIF1α and PKM2, cooperate to induce glycolysis in M1 macrophages (Izquierdo et al., 2015; Palsson-McDermott et al., 2015). The reason why iNOS inhibition induces glycolysis remains unstudied, but it might be attributable to glyceraldehyde-3-phosphate dehydrogenase activation. Indeed, NO induces ADP ribosylation of this glycolytic enzyme and thereby inhibits its activity (Dimmeler and Brüne, 1993).

Although iNOS inhibition clearly improved mitochondrial function in M1 cells, it only partially restored M1→M2 repolarization, highlighting the existence of additional mechanisms that prevent the conversion of inflammatory macrophages into anti-inflammatory cells. In support of this notion, human M1 macrophages did not secrete NO in vitro (data not shown), and, thus, additional unidentified mechanisms are clearly at play that prevent M1→M2 repolarization in mice and humans. Possibly itaconate contributes to the suppression of mitochondrial function in inflammatory macrophages. This antibacterial product is highly induced by inflammatory stimuli in both mouse and human macrophages, and it has been reported to impair the activity of complex II of the electron transport chain (Meiser et al., 2016; Michelucci et al., 2013; O'Neill and Pearce, 2016). In patients, however, iNOS$^+$ macrophages are present in a variety of inflammatory diseases, and NO might therefore also impair M1→M2 repolarization in vivo in humans (Bingisser and Holt, 2001; Stöger et al., 2012; Thomas and Mattila, 2014).

Our findings support the earlier notion that M1 macrophages are end-stage killer cells (Italiani and Boraschi, 2014). Accordingly, neutrophils show an M1-like metabolism with high glycolysis and low OXPHOS. Their metabolism underlies the uniting characteristic of granulocytes, and these inflammatory phagocytes are short lived and terminally differentiated (Pearce and Pearce, 2013). Indeed, M1 cells failed to adopt an M2 phenotype during an IL-4 challenge in vivo. These observations imply that the apparent switch from M1 to M2 macrophages during the course of infection or healing responses is probably not caused by actual M1→M2 repolarization of the macrophages that are present, but rather by the repopulation and M2 polarization of newly recruited blood monocytes in the healing-promoting environment, as suggested previously (Italiani and Boraschi, 2014). The observation that inhibition or deletion of iNOS improves M1→M2 repolarization, without affecting M1 or M2 polarization as such, could help to explain previous in vivo findings in *Nos2*$^{-/-}$ mice. Indeed, improved reprogramming of pro-atherogenic M1 cells to inflammation-resolving, pro-fibrotic M2 macrophages may underlie the decreased atherosclerosis (Kuhlencordt et al., 2001) and increased atherosclerotic collagen deposition (Niu et al., 2001) observed in *Nos2*$^{-/-}$ mice.

Our thorough metabolic characterization of polarized and repolarized macrophages not only explains why M1 cells fail to repolarize to M2 but also simultaneously clarifies why M2 macrophages are highly plastic and readily repolarize to M1. Indeed, while exhibiting a modest basal glycolytic rate, M2 macrophages display high glycolytic reserves and immediately switch to high glycolysis after mitochondrial ATP production is blocked. How mitochondrial oxidative metabolism supports IL-4-induced polarization, as demonstrated here and by others (Tan et al., 2015; Vats et al., 2006), remains elusive and deserves further investigation. In this context, we are currently investigating how metabolic changes affect metabolite availability for epigenetic enzymes and, through epigenetic remodeling, influence M1- and M2-associated gene expression (Baardman et al., 2015).

Overall, the present study demonstrates that M1 activation of macrophages blunts OXPHOS, thereby preventing their repolarization to M2. Restoring mitochondrial function, for example, through iNOS inhibition, might be useful to improve the reprogramming of M1 into M2 macrophages as a method of controlling inflammatory diseases.

EXPERIMENTAL PROCEDURES

Mice

Wild-type C57BL/6J(c) and B6.SJL-*Ptprc*^{a} *Pepc*^{b}/BoyJ (CD45.1$^+$) 8- to 16-week-old mice were obtained from Charles River Laboratories, and bone marrow of *Nos2*$^{-/-}$ mice (B6.129P2-*Nos2*^{tm1Lau}/J) was a gift from Claude Libert (VIB, Ghent University). All experiments were approved by the Committee for Animal Welfare (University of Amsterdam).

Macrophage Cultures

Mouse bone marrow cells were isolated and cultured in RPMI-1640 with 2 mM L-glutamine, 10% fetal calf serum (FCS), penicillin (100 U/mL), streptomycin (100 μg/mL) (Gibco), and 15% L929-conditioned medium. Human peripheral mononuclear blood cells were isolated from healthy donors by density centrifugation using Lymphoprep (Axis-Shield). Next, monocytes were purified by magnetic-activated cell separation using human anti-CD14 beads and LS separation columns (Miltenyi). Cells were cultured in Iscove's modified Dulbecco's medium (IMDM, Life Technologies) with 10% FCS, penicillin (100 U/mL), streptomycin (100 μg/mL) (Gibco), and 25 ng/mL human macrophage-colony stimulating factor (M-CSF, Miltenyi) at 10^6 cells/mL. On day 6, cells were harvested, seeded at 10^6 cells/mL, and stimulated 24 hr with 10 U/mL IFNγ (PeproTech) + 10 ng/ml LPS (Sigma-Aldrich) or 100 U/mL IL-4 (Peprotech) to elicit M1 or M2 cells, respectively. The 100 U/mL IL-10 (PeproTech) was used to elicit another type of M2-like macrophage. For repolarization, BMMs were primed with IL-4 or LPS + IFNγ or they were left untreated. After 24 hr, cells were washed and treated with the opposing stimulus for another 24 hr. OM (2 μM), 2-DG (1 mM), ETO (50 μM), 1400W (100 μM), or NAC (5 mM) (all Sigma-Aldrich) was added 30 min before macrophage activation.

In Vivo Macrophage (Re)polarization

To assess in vivo M1→M2 repolarization after IL-4 injection, BMMs from CD45.1 donor mice were stimulated ex vivo with LPS + IFNγ or left untreated. After 24 hr, these CD45.1$^+$ macrophages were harvested, washed in PBS, counted, analyzed for their M1 phenotype, and injected (2.5 × 10^6 cells per mouse) intraperitoneally into C57BL/6J(c) (CD45.2$^+$) acceptor mice that next received IL-4 (or PBS as control). To optimize the effect of IL-4, it was administered as an IL-4/anti-IL-4 complex (IL-4c), consisting of 5 μg recombinant mouse IL-4 (PeproTech) and 25 μg 11B11 anti-IL-4 (BioConnect) in 100 μl PBS, as described previously (Jenkins et al., 2013). Then 48 hr after the IL-4 challenge, peritoneal cells were collected and analyzed by flow cytometry.

Gene Expression Analysis

RNA was isolated with High Pure RNA Isolation kits (Roche), cDNA was synthesized with iScript (Bio-Rad), and qPCR was performed using Sybr Green Fast mix (Applied Biosytems) on a ViiA7 (Applied Biosystems).

Housekeeping genes *Rplp0* (Arbp) and *Ppia* were used for normalization. Primer sequences are available upon request.

Flow Cytometry

Cells were pre-incubated with Fc-block followed by the labeling antibodies listed in Table S2. Cell viability was assessed by PI/Annexin V-Alexa-Fluor647 staining according to the manufacturer's protocol (Invitrogen). Data were acquired with a FACSCantoII (Becton Dickinson) and analyzed using FlowJo (Tree Star). Surface expression was calculated as ΔMFI = (Median fluorescence intensity)$_{\text{positive staining}}$ – (Median fluorescence intensity)$_{\text{isotype staining}}$.

Macrophage Function

IL-6, IL-12(p40), and TNF were quantified by ELISA in accordance with the supplier's protocols (Life Technologies). NO production was measured by NO_2^- quantification in a Griess reaction (Sigma-Aldrich). 2',7' –dichlorofluorescin diacetate (DCFDA) was used to measure ROS and oxidative stress was measured with CellROX (both Thermo Fisher Scientific). Arginase activity (1 U = amount of enzyme that catalyzes the formation of 1 μmol urea/min/10^6 cells) was assessed as described previously (Van den Bossche et al., 2012).

Immunoblotting

BMM lysates were separated on a NuPAGE Novex 4%–12% Bis-Tris gel (Thermo Fisher Scientific) and transferred onto nitrocellulose membrane (Bio-Rad). After blocking, membranes were incubated with primary antibodies (Table S2), followed by incubation with horseradish peroxidase (HRP)-conjugated secondary antibodies and visualization using the SuperSignal West Pico Chemiluminescent Substrate (Thermo Fisher Scientific).

MTT Assay

Succinate dehydrogenase activity was assessed by yellow MTT reduction into purple formazan. Macrophages were incubated with 1 mg/mL MTT (Sigma-Aldrich) for 3 hr, lysed with 0.1 N HCl in isopropanol, and the released solubilized formazan was measured spectrophotometrically and compared to the levels in naive macrophages (N = 100%).

Metabolic Extracellular Flux Analysis

BMMs (25,000) were plated in XF-96-cell culture plates (Seahorse Bioscience) and treated as indicated. ECARs and OCRs were measured in an XF-96 Flux Analyzer (Seahorse Bioscience) as described previously (Van den Bossche et al., 2015). Changes in ECAR in response to glucose, OM, and 2-DG injection were used to calculate all glycolysis parameters, and OXPHOS characteristics were calculated from the OCR changes in response to OM, FCCP, and ROT + AA injection, as detailed in Figure S3. FAO was measured as described previously (Zhang et al., 2012). In brief, 200 μM palmitate-BSA complex was injected into XF-96-cell culture plates containing naive, M1, or M2 macrophages. Next, the fraction of OCR attributed to palmitate oxidation was determined by ETO (100 μM) injection and calculated as FAO = $OCR_{\text{before ETO}}$ – $OCR_{\text{after ETO}}$. The activity of the individual mitochondrial respiratory complexes I–IV was measured using an established protocol (Salabei et al., 2014). In brief, plasma membrane-permeabilized (PMP) macrophages were treated with a cocktail of specific substrates and inhibitors (all from Sigma-Aldrich; Table S1) to measure complex I-, II-, III-, and IV-mediated OCR. On completion of the distinct Seahorse experiments, DNA content was measured with CyQuant to normalize ECAR and OCR data.

Statistics

Data were evaluated with GraphPad Prism 4 using one-way ANOVA. Unless otherwise stated, values represent the mean ± SEM of three replicates of one representative experiment (*$p < 0.05$, **$p < 0.01$, and ***$p < 0.001$).

SUPPLEMENTAL INFORMATION

Supplemental Information includes eight figures and two tables and can be found with this article online at http://dx.doi.org/10.1016/j.celrep.2016.09.008.

AUTHOR CONTRIBUTIONS

Conceptualization, J.V.d.B.; Methodology, J.V.d.B.; Formal Analysis, J.V.d.B., J.B., and N.A.O.; Investigation, J.V.d.B., J.B., N.A.O., S.v.d.V., A.E.N., S.M.v.d.B., R.L.-M., H.-J.C., M.C.S.B., M.A., M.A.H., and A.F.d.V.; Writing – Original Draft, J.V.d.B.; Writing – Review & Editing, J.V.d.B. and M.P.J.d.W.; Visualization, J.V.d.B.; Supervision, J.V.d.B. and M.P.J.d.W.; Funding Acquisition, J.V.d.B.

ACKNOWLEDGMENTS

J.V.d.B. received a VENI grant from ZonMW (91615052) and a Netherlands Heart Foundation Junior Postdoctoral grant (2013T003). M.P.J.d.W. is an Established Investigator of the Netherlands Heart Foundation (2007T067), is supported by Netherlands Heart Foundation grant 2010B022, and holds an Academic Medical Center (AMC) fellowship. We also acknowledge the support from the Netherlands CardioVascular Research Initiative, Dutch Federation of University Medical Centers, the Netherlands Organization for Health Research and Development, and the Royal Netherlands Academy of Sciences for the GENIUS project "Generating the best evidence-based pharmaceutical targets for atherosclerosis" (CVON2011-19).

Received: May 10, 2016
Revised: July 27, 2016
Accepted: September 1, 2016
Published: October 11, 2016

REFERENCES

Albina, J.E., and Mastrofrancesco, B. (1993). Modulation of glucose metabolism in macrophages by products of nitric oxide synthase. Am. J. Physiol. *264*, C1594–C1599.

Allavena, P., Peccatori, F., Maggioni, D., Erroi, A., Sironi, M., Colombo, N., Lissoni, A., Galazka, A., Meiers, W., Mangioni, C., et al. (1990). Intraperitoneal recombinant gamma-interferon in patients with recurrent ascitic ovarian carcinoma: modulation of cytotoxicity and cytokine production in tumor-associated effectors and of major histocompatibility antigen expression on tumor cells. Cancer Res. *50*, 7318–7323.

Baardman, J., Licht, I., de Winther, M.P., and Van den Bossche, J. (2015). Metabolic-epigenetic crosstalk in macrophage activation. Epigenomics *7*, 1155–1164.

Bingisser, R.M., and Holt, P.G. (2001). Immunomodulating mechanisms in the lower respiratory tract: nitric oxide mediated interactions between alveolar macrophages, epithelial cells, and T-cells. Swiss Med. Wkly. *131*, 171–179.

Brown, G.C., and Borutaite, V. (2007). Nitric oxide and mitochondrial respiration in the heart. Cardiovasc. Res. *75*, 283–290.

Chénais, B., Morjani, H., and Drapier, J.C. (2002). Impact of endogenous nitric oxide on microglial cell energy metabolism and labile iron pool. J. Neurochem. *81*, 615–623.

Colombo, N., Peccatori, F., Paganin, C., Bini, S., Brandely, M., Mangioni, C., Mantovani, A., and Allavena, P. (1992). Anti-tumor and immunomodulatory activity of intraperitoneal IFN-gamma in ovarian carcinoma patients with minimal residual tumor after chemotherapy. Int. J. Cancer *51*, 42–46.

Cramer, T., Yamanishi, Y., Clausen, B.E., Förster, I., Pawlinski, R., Mackman, N., Haase, V.H., Jaenisch, R., Corr, M., Nizet, V., et al. (2003). HIF-1alpha is essential for myeloid cell-mediated inflammation. Cell *112*, 645–657.

Das, A., Sinha, M., Datta, S., Abas, M., Chaffee, S., Sen, C.K., and Roy, S. (2015). Monocyte and macrophage plasticity in tissue repair and regeneration. Am. J. Pathol. *185*, 2596–2606.

Davis, M.J., Tsang, T.M., Qiu, Y., Dayrit, J.K., Freij, J.B., Huffnagle, G.B., and Olszewski, M.A. (2013). Macrophage M1/M2 polarization dynamically adapts to changes in cytokine microenvironments in Cryptococcus neoformans infection. MBio *4*, e00264-13.

Dimmeler, S., and Brüne, B. (1993). Nitric oxide preferentially stimulates auto-ADP-ribosylation of glyceraldehyde-3-phosphate dehydrogenase compared to alcohol or lactate dehydrogenase. FEBS Lett. *315*, 21–24.

Everts, B., Amiel, E., van der Windt, G.J., Freitas, T.C., Chott, R., Yarasheski, K.E., Pearce, E.L., and Pearce, E.J. (2012). Commitment to glycolysis sustains survival of NO-producing inflammatory dendritic cells. Blood *120*, 1422–1431.

Galván-Peña, S., and O'Neill, L.A. (2014). Metabolic reprograming in macrophage polarization. Front. Immunol. *5*, 420.

Garvey, E.P., Oplinger, J.A., Furfine, E.S., Kiff, R.J., Laszlo, F., Whittle, B.J., and Knowles, R.G. (1997). 1400W is a slow, tight binding, and highly selective inhibitor of inducible nitric-oxide synthase in vitro and in vivo. J. Biol. Chem. *272*, 4959–4963.

Gordon, S., and Martinez, F.O. (2010). Alternative activation of macrophages: mechanism and functions. Immunity *32*, 593–604.

Hagemann, T., Lawrence, T., McNeish, I., Charles, K.A., Kulbe, H., Thompson, R.G., Robinson, S.C., and Balkwill, F.R. (2008). "Re-educating" tumor-associated macrophages by targeting NF-kappaB. J. Exp. Med. *205*, 1261–1268.

Huang, S.C., Everts, B., Ivanova, Y., O'Sullivan, D., Nascimento, M., Smith, A.M., Beatty, W., Love-Gregory, L., Lam, W.Y., O'Neill, C.M., et al. (2014). Cell-intrinsic lysosomal lipolysis is essential for alternative activation of macrophages. Nat. Immunol. *15*, 846–855.

Italiani, P., and Boraschi, D. (2014). From monocytes to M1/M2 macrophages: phenotypical vs. functional differentiation. Front. Immunol. *5*, 514.

Izquierdo, E., Cuevas, V.D., Fernández-Arroyo, S., Riera-Borrull, M., Orta-Zavalza, E., Joven, J., Rial, E., Corbi, A.L., and Escribese, M.M. (2015). Reshaping of human macrophage polarization through modulation of glucose catabolic pathways. J. Immunol. *195*, 2442–2451.

Jenkins, S.J., Ruckerl, D., Thomas, G.D., Hewitson, J.P., Duncan, S., Brombacher, F., Maizels, R.M., Hume, D.A., and Allen, J.E. (2013). IL-4 directly signals tissue-resident macrophages to proliferate beyond homeostatic levels controlled by CSF-1. J. Exp. Med. *210*, 2477–2491.

Jha, A.K., Huang, S.C., Sergushichev, A., Lampropoulou, V., Ivanova, Y., Loginicheva, E., Chmielewski, K., Stewart, K.M., Ashall, J., Everts, B., et al. (2015). Network integration of parallel metabolic and transcriptional data reveals metabolic modules that regulate macrophage polarization. Immunity *42*, 419–430.

Khallou-Laschet, J., Varthaman, A., Fornasa, G., Compain, C., Gaston, A.T., Clement, M., Dussiot, M., Levillain, O., Graff-Dubois, S., Nicoletti, A., and Caligiuri, G. (2010). Macrophage plasticity in experimental atherosclerosis. PLoS ONE *5*, e8852.

Kuhlencordt, P.J., Chen, J., Han, F., Astern, J., and Huang, P.L. (2001). Genetic deficiency of inducible nitric oxide synthase reduces atherosclerosis and lowers plasma lipid peroxides in apolipoprotein E-knockout mice. Circulation *103*, 3099–3104.

Martinez, F.O., Helming, L., Milde, R., Varin, A., Melgert, B.N., Draijer, C., Thomas, B., Fabbri, M., Crawshaw, A., Ho, L.P., et al. (2013). Genetic programs expressed in resting and IL-4 alternatively activated mouse and human macrophages: similarities and differences. Blood *121*, e57–e69.

Meiser, J., Krämer, L., Sapcariu, S.C., Battello, N., Ghelfi, J., D'Herouel, A.F., Skupin, A., and Hiller, K. (2016). Pro-inflammatory macrophages sustain pyruvate oxidation through pyruvate dehydrogenase for the synthesis of itaconate and to enable cytokine expression. J. Biol. Chem. *291*, 3932–3946.

Michelucci, A., Cordes, T., Ghelfi, J., Pailot, A., Reiling, N., Goldmann, O., Binz, T., Wegner, A., Tallam, A., Rausell, A., et al. (2013). Immune-responsive gene 1 protein links metabolism to immunity by catalyzing itaconic acid production. Proc. Natl. Acad. Sci. USA *110*, 7820–7825.

Munder, M., Eichmann, K., and Modolell, M. (1998). Alternative metabolic states in murine macrophages reflected by the nitric oxide synthase/arginase balance: competitive regulation by CD4+ T cells correlates with Th1/Th2 phenotype. J. Immunol. *160*, 5347–5354.

Murray, P.J., Allen, J.E., Biswas, S.K., Fisher, E.A., Gilroy, D.W., Goerdt, S., Gordon, S., Hamilton, J.A., Ivashkiv, L.B., Lawrence, T., et al. (2014). Macrophage activation and polarization: nomenclature and experimental guidelines. Immunity *41*, 14–20.

Namgaladze, D., and Brüne, B. (2014). Fatty acid oxidation is dispensable for human macrophage IL-4-induced polarization. Biochim. Biophys. Acta *1841*, 1329–1335.

Niu, X.L., Yang, X., Hoshiai, K., Tanaka, K., Sawamura, S., Koga, Y., and Nakazawa, H. (2001). Inducible nitric oxide synthase deficiency does not affect the susceptibility of mice to atherosclerosis but increases collagen content in lesions. Circulation *103*, 1115–1120.

Nomura, M., Liu, J., Rovira, I.I., Gonzalez-Hurtado, E., Lee, J., Wolfgang, M.J., and Finkel, T. (2016). Fatty acid oxidation in macrophage polarization. Nat. Immunol. *17*, 216–217.

O'Neill, L.A., and Pearce, E.J. (2016). Immunometabolism governs dendritic cell and macrophage function. J. Exp. Med. *213*, 15–23.

Okabe, Y., and Medzhitov, R. (2016). Tissue biology perspective on macrophages. Nat. Immunol. *17*, 9–17.

Ouimet, M., Ediriweera, H.N., Gundra, U.M., Sheedy, F.J., Ramkhelawon, B., Hutchison, S.B., Rinehold, K., van Solingen, C., Fullerton, M.D., Cecchini, K., et al. (2015). MicroRNA-33-dependent regulation of macrophage metabolism directs immune cell polarization in atherosclerosis. J. Clin. Invest. *125*, 4334–4348.

Palsson-McDermott, E.M., Curtis, A.M., Goel, G., Lauterbach, M.A., Sheedy, F.J., Gleeson, L.E., van den Bosch, M.W., Quinn, S.R., Domingo-Fernandez, R., Johnston, D.G., et al. (2015). Pyruvate kinase M2 regulates Hif-1α activity and IL-1β induction and is a critical determinant of the warburg effect in LPS-activated macrophages. Cell Metab. *21*, 65–80.

Pearce, E.L., and Pearce, E.J. (2013). Metabolic pathways in immune cell activation and quiescence. Immunity *38*, 633–643.

Raza, H., John, A., and Shafarin, J. (2014). NAC attenuates LPS-induced toxicity in aspirin-sensitized mouse macrophages via suppression of oxidative stress and mitochondrial dysfunction. PLoS ONE *9*, e103379.

Rigamonti, E., Zordan, P., Sciorati, C., Rovere-Querini, P., and Brunelli, S. (2014). Macrophage plasticity in skeletal muscle repair. BioMed Res. Int. *2014*, 560629.

Salabei, J.K., Gibb, A.A., and Hill, B.G. (2014). Comprehensive measurement of respiratory activity in permeabilized cells using extracellular flux analysis. Nat. Protoc. *9*, 421–438.

Sica, A., and Mantovani, A. (2012). Macrophage plasticity and polarization: in vivo veritas. J. Clin. Invest. *122*, 787–795.

Stöger, J.L., Gijbels, M.J., van der Velden, S., Manca, M., van der Loos, C.M., Biessen, E.A., Daemen, M.J., Lutgens, E., and de Winther, M.P. (2012). Distribution of macrophage polarization markers in human atherosclerosis. Atherosclerosis *225*, 461–468.

Tan, Z., Xie, N., Cui, H., Moellering, D.R., Abraham, E., Thannickal, V.J., and Liu, G. (2015). Pyruvate dehydrogenase kinase 1 participates in macrophage polarization via regulating glucose metabolism. J. Immunol. *194*, 6082–6089.

Tannahill, G.M., Curtis, A.M., Adamik, J., Palsson-McDermott, E.M., McGettrick, A.F., Goel, G., Frezza, C., Bernard, N.J., Kelly, B., Foley, N.H., et al. (2013). Succinate is an inflammatory signal that induces IL-1β through HIF-1α. Nature *496*, 238–242.

Thomas, A.C., and Mattila, J.T. (2014). "Of mice and men": arginine metabolism in macrophages. Front. Immunol. *5*, 479.

Van den Bossche, J., Bogaert, P., van Hengel, J., Guérin, C.J., Berx, G., Movahedi, K., Van den Bergh, R., Pereira-Fernandes, A., Geuns, J.M., Pircher, H., et al. (2009). Alternatively activated macrophages engage in homotypic and heterotypic interactions through IL-4 and polyamine-induced E-cadherin/catenin complexes. Blood *114*, 4664–4674.

Van den Bossche, J., Lamers, W.H., Koehler, E.S., Geuns, J.M., Alhonen, L., Uimari, A., Pirnes-Karhu, S., Van Overmeire, E., Morias, Y., Brys, L., et al. (2012). Pivotal advance: Arginase-1-independent polyamine production stimulates the expression of IL-4-induced alternatively activated macrophage markers while inhibiting LPS-induced expression of inflammatory genes. J. Leukoc. Biol. *91*, 685–699.

Van den Bossche, J., Baardman, J., and de Winther, M.P. (2015). Metabolic characterization of polarized M1 and M2 bone marrow-derived macrophages using real-time extracellular flux analysis. J. Vis. Exp. *105*.

Vats, D., Mukundan, L., Odegaard, J.I., Zhang, L., Smith, K.L., Morel, C.R., Wagner, R.A., Greaves, D.R., Murray, P.J., and Chawla, A. (2006). Oxidative metabolism and PGC-1beta attenuate macrophage-mediated inflammation. Cell Metab. *4*, 13–24.

Wynn, T.A., Chawla, A., and Pollard, J.W. (2013). Macrophage biology in development, homeostasis and disease. Nature *496*, 445–455.

Xue, J., Schmidt, S.V., Sander, J., Draffehn, A., Krebs, W., Quester, I., De Nardo, D., Gohel, T.D., Emde, M., Schmidleithner, L., et al. (2014). Transcriptome-based network analysis reveals a spectrum model of human macrophage activation. Immunity *40*, 274–288.

Zhang, J., Nuebel, E., Wisidagama, D.R., Setoguchi, K., Hong, J.S., Van Horn, C.M., Imam, S.S., Vergnes, L., Malone, C.S., Koehler, C.M., and Teitell, M.A. (2012). Measuring energy metabolism in cultured cells, including human pluripotent stem cells and differentiated cells. Nat. Protoc. *7*, 1068–1085.

Cell Reports, Volume *17*

Supplemental Information

Mitochondrial Dysfunction Prevents Repolarization of Inflammatory Macrophages

Jan Van den Bossche, Jeroen Baardman, Natasja A. Otto, Saskia van der Velden, Annette E. Neele, Susan M. van den Berg, Rosario Luque-Martin, Hung-Jen Chen, Marieke C.S. Boshuizen, Mohamed Ahmed, Marten A. Hoeksema, Alex F. de Vos, and Menno P.J. de Winther

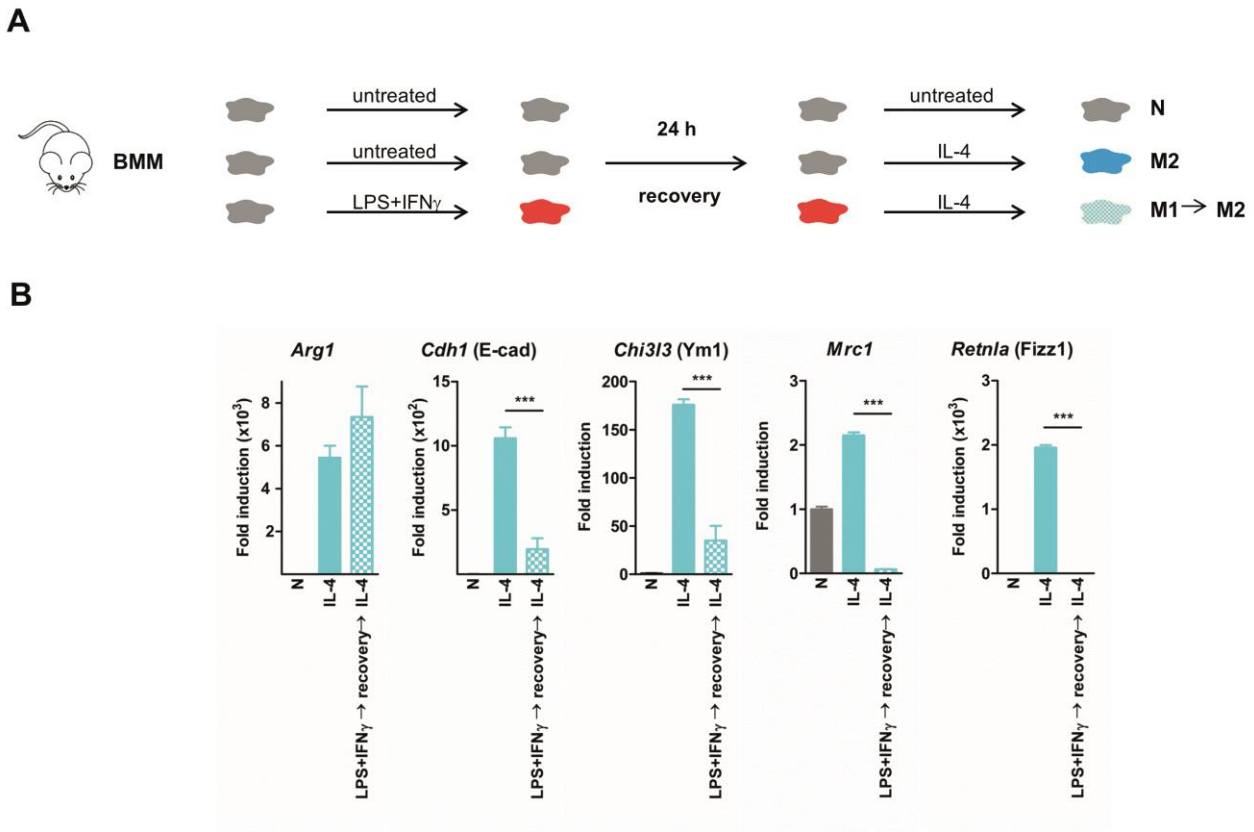

Figure S1. 24 h recovery between the first LPS+IFNγ -induced inflammatory storm and the subsequent IL-4 treatment does not improve M2 repolarization. **Related to Figure 1. (A)** To assess whether the M1-induced impairment of M2 repolarization has long-term effects, we now allowed the macrophages to recover for 24 h between the M1 stimulation and the subsequent M2 restimulation. **(B)** The fold inductions of indicated IL-4-induced M2 marker genes are shown relative to the expression in untreated macrophages (=1). Values represent mean ± SEM of 3 mice. ****P*<.001.

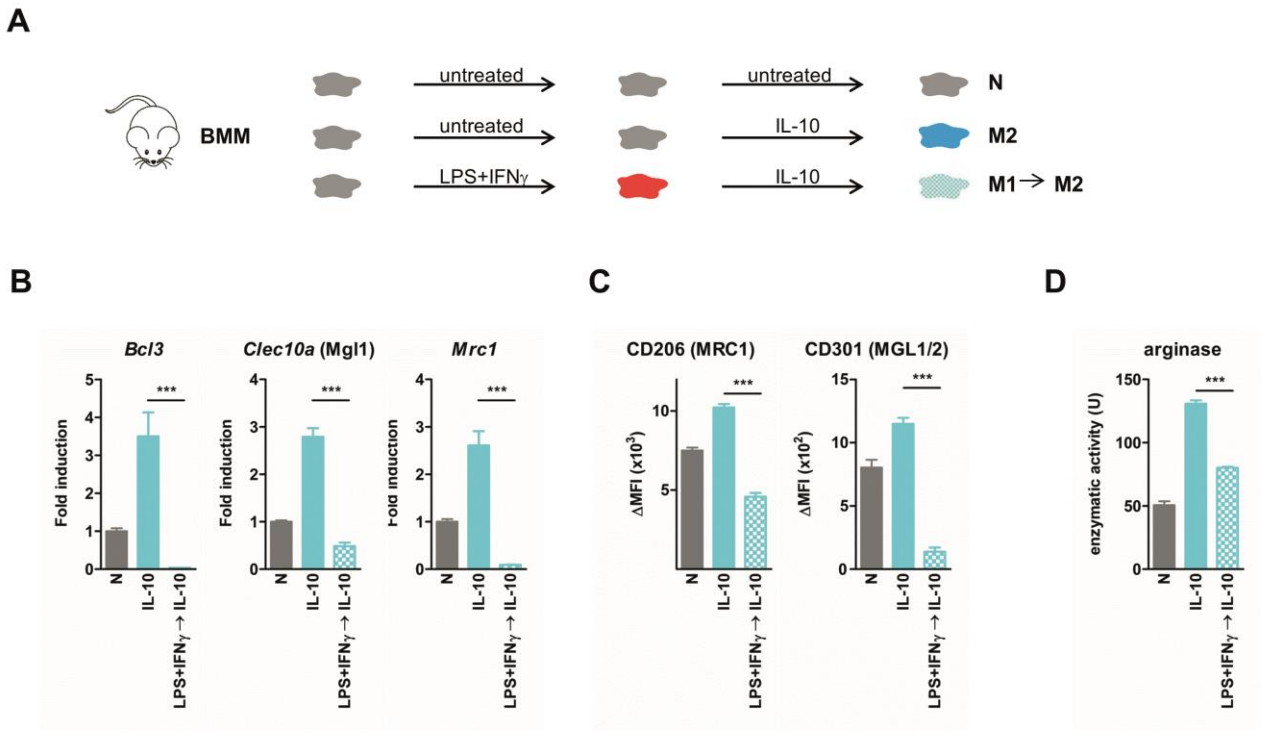

Figure S2. LPS+IFNγ-primed mouse M1 macrophages fail to repolarize to M2-like cells upon IL-10 restimulation. **Related to Figure 1. (A)** Normal IL-10-elicited M2 macrophages were compared to M1→M2 macrophages that were primed for 24 h with LPS+IFNγ before 24 h IL-10 stimulation. **(B)** The fold inductions of indicated IL-10-induced genes are shown relative to the expression in untreated macrophages (=1). **(C)** Differentially treated macrophages were stained with antibodies against the M2 surface markers CD206 (MRC1, mannose receptor C type 1), CD301 (MGL1/2, macrophage galactose-binding lectin) or isotype control, followed by flow cytometric analysis. Surface expression levels (ΔMFI = $[\text{Median fluorescence intensity}]_{\text{positive staining}} - [\text{Median fluorescence intensity}]_{\text{isotype staining}}$) are presented. **(D)** Arginase activity in BMM lysates was measured and shown as units (U) enzymatic activity. Values represent mean ± SEM of 3 mice. ****P*<.001.

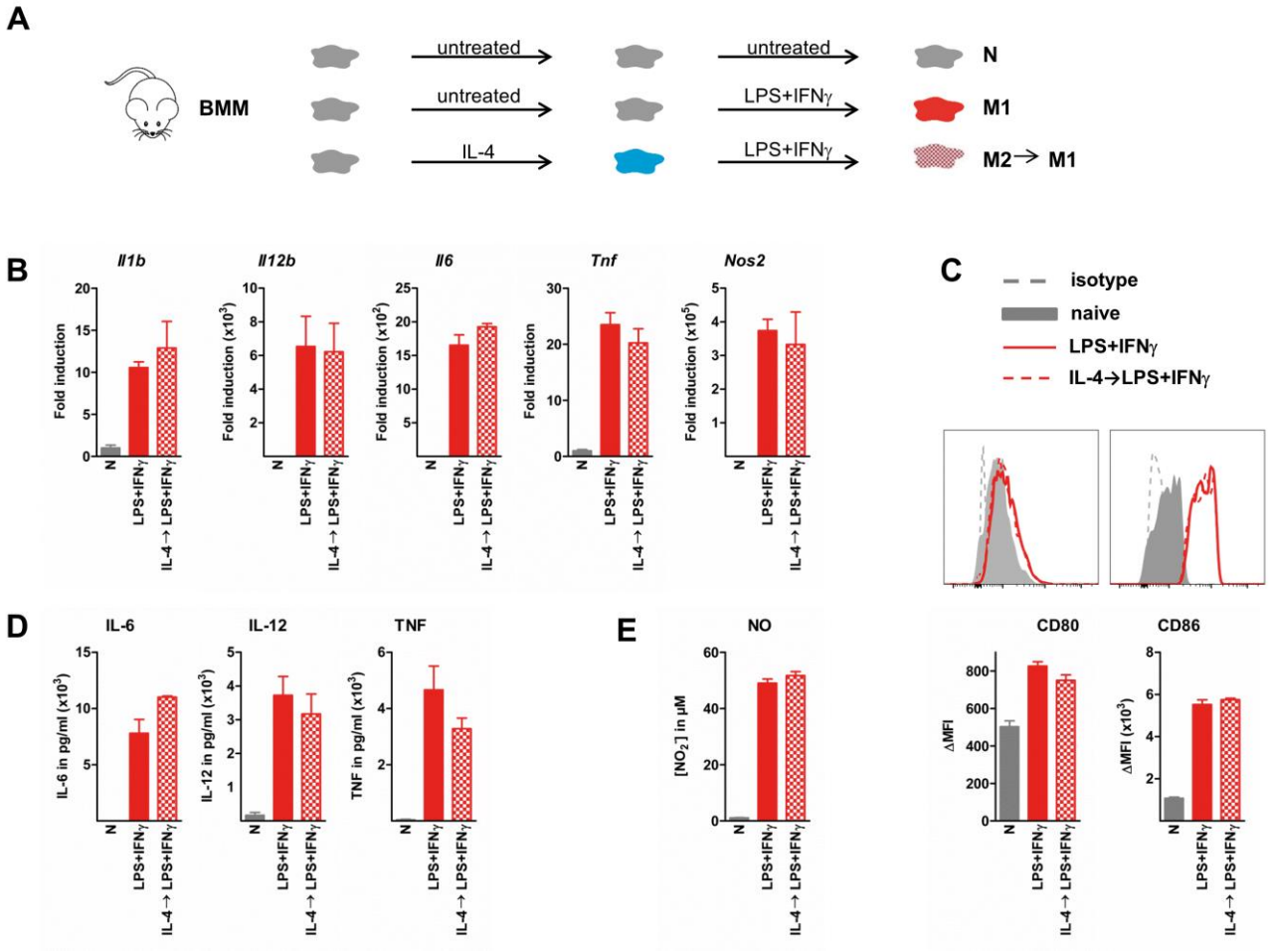

Figure S3. IL-4-induced M2 macrophages readily respond to LPS+IFNγ-stimulation and accept an inflammatory M1-like phenotype. **Related to Figure 1. (A)** To study the plasticity of M2 macrophages, mouse BMMs were primed with IL-4, or were left untreated. After 24 h, cells were washed and treated with LPS+IFNγ for another 24 h, or remained untreated as control. LPS+IFNγ-induced M1 macrophages were compared to M2→M1 macrophages that were primed with IL-4 before LPS+IFNγ treatment. **(B)** The fold inductions of indicated M1-associated inflammatory genes are shown relative to the expression in untreated macrophages (=1). **(C)** (Re)polarized macrophages were stained with antibodies against CD80, CD86 or isotype control, followed by flow cytometric analysis. Representative histogram overlays for differentially treated macrophages, together with the quantified surface expression values (ΔMFI = [Median fluorescence intensity]$_{\text{positive staining}}$ – [Median fluorescence intensity]$_{\text{isotype staining}}$) are shown. **(D-E)** Cytokine and NO concentrations in BMM culture supernatant are presented as measured by ELISA and Griess reaction, respectively. Values represent mean ± SEM of 3 mice.**P*<.05; ***P*<.01; ****P*<.001; ns = not significant.

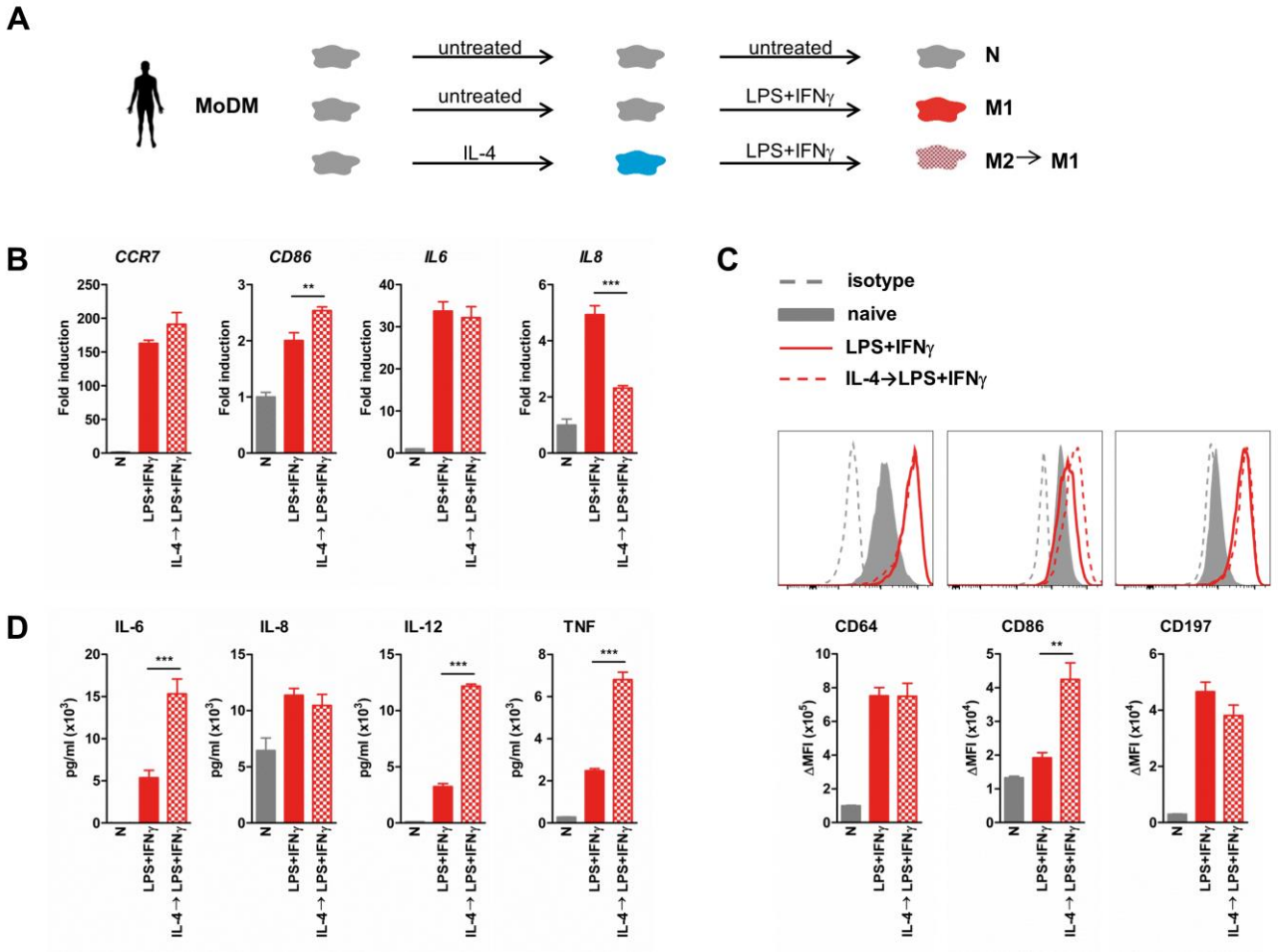

Figure S4. Human IL-4-induced M2 macrophages efficiently respond to LPS+IFNγ-stimulation to accept an inflammatory phenotype. **Related to Figure 2. (A)** To study the plasticity of human M2 macrophages, peripheral blood monocyte-derived macrophages (MoDM)s were primed with IL-4, or were left untreated. After 24 h, cells were washed and treated with LPS+IFNγ for another 24 h, or remained untreated as control. LPS+IFNγ-induced M1 macrophages were compared to M2→M1 macrophages that were primed with IL-4 before LPS+IFNγ treatment. **(B)** The fold inductions of indicated M1-associated inflammatory genes are shown relative to the expression in untreated macrophages (=1). **(C)** (Re)polarized macrophages were stained with antibodies against human CD14, CD197 (CCR7), CD64, CD86, or isotype control, followed by flow cytometric analysis. Representative histogram overlays for differentially treated $CD14^+$ macrophages, together with the quantified surface expression values (ΔMFI = $[\text{Median fluorescence intensity}]_{\text{positive staining}} - [\text{Median fluorescence intensity}]_{\text{isotype staining}}$) are shown. **(D)** Cytokine concentrations in human MoDM culture supernatant are presented as measured by ELISA. Values represent mean ± SEM of 3 wells of one representative donor (out of 3 tested donors).*P<.05; **P<.01; ***P<.001; ns = not significant.

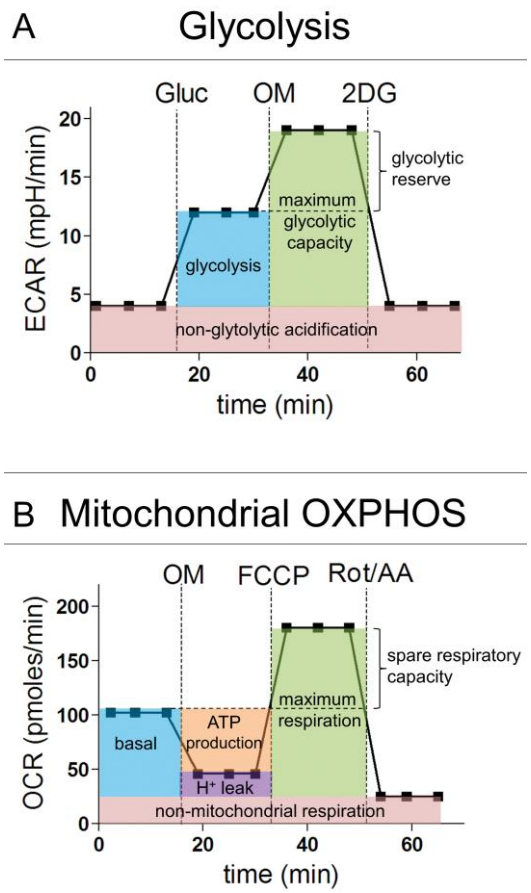

Figure S5. Metabolic parameters derived from an extracellular flux assay. **Related to Figure 4. (A)** After the injection of glucose (gluc), the increase in extracellular acidification rate (ECAR in mpH/min) represents the glycolysis rate. The additional increase in ECAR after ATP synthase inhibition with oligomycin (OM) provides information about the glycolytic reserve and capacity. **(B)** When analysing the oxygen consumption rates (OCR in pMoles/min), OM injection allows to calculate the oxygen consumption used for mitochondrial ATP synthesis. Carbonyl cyanide 4-(trifluoromethoxy)phenylhydrazone (FCCP) uncouples mitochondrial respiration and the corresponding OCR measurements yield data about the maximal and spare respiratory capacity. Finally, injection of rotenone (Rot) and antimycin A (AA) block mitochondrial complex I and III and the residual OCR represents the non-mitochondrial oxygen consumption. After normalization for cell counts with CyQUANT, following metabolic parameters are calculated as follows:

Glycolysis = avg. $ECAR_{(4,5,6)}$ – avg. $ECAR_{(1,2,3)}$

Maximum glycolytic capacity = avg. $ECAR_{(7,8,9)}$ – avg. $ECAR_{(1,2,3)}$

Glycolytic reserve= avg. $ECAR_{(7,8,9)}$ - avg. $ECAR_{(4,5,6)}$

Basal respiration = avg. $OCR_{(1,2,3)}$ - avg. $OCR_{(10,11,12)}$

ATP production = avg. $OCR_{(1,2,3)}$ - avg. $OCR_{(4,5,6)}$

Maximum respiration = avg. $OCR_{(7,8,9)}$ - avg. $OCR_{(10,11,12)}$

Spare respiratory capacity (SRC) = avg. $OCR_{(7,8,9)}$ - avg. $OCR_{(1,2,3)}$

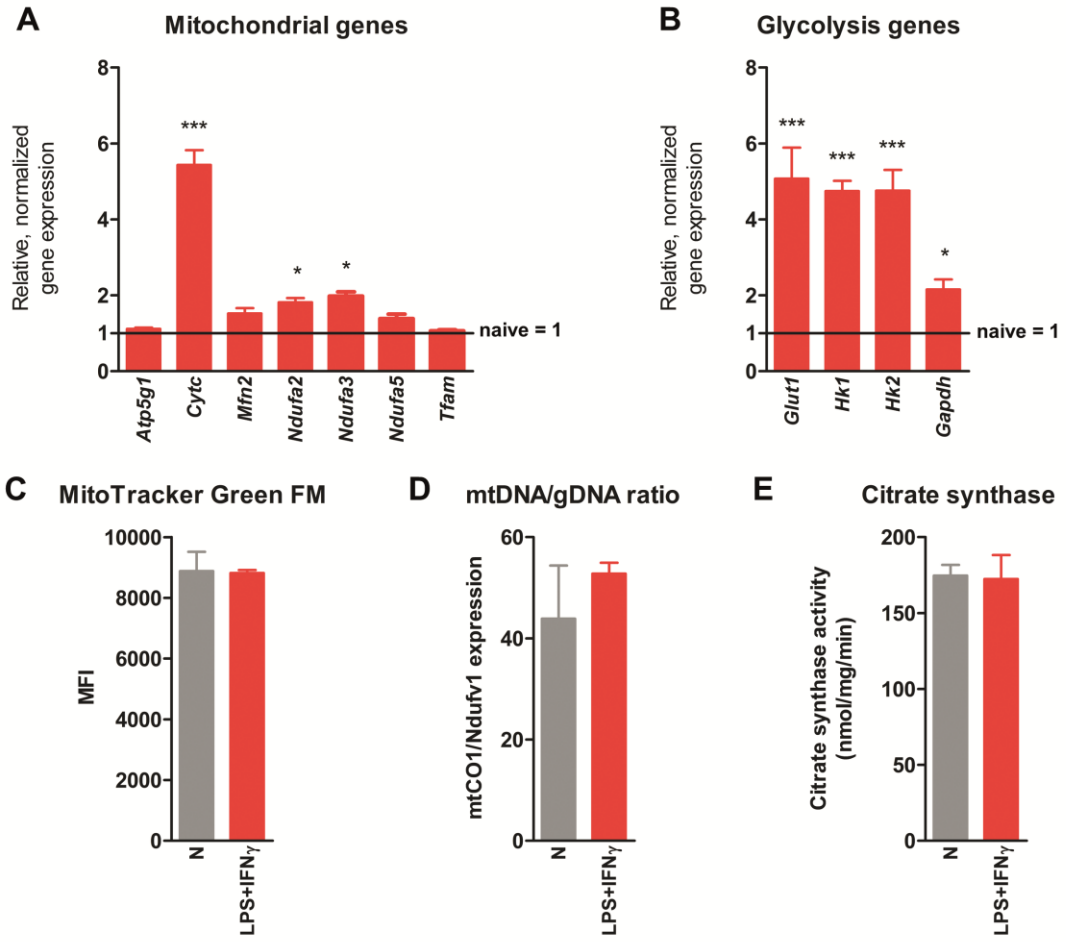

Figure S6. Suppressed OXPHOS in M1 cells is not caused by reduced expression of mitochondrial genes, nor by reduced mitochondrial mass, nor by reduced citrate synthase activity. Related to Figure 4. To understand the mechanism of reduced mitochondrial oxygen consumption in M1, we first studied the effect of LPS+IFNγ treatment on a broad set of **(A)** mitochondrial and **(B)** glycolysis genes. The fold inductions of indicated genes are shown relative to the expression in untreated macrophages (naive=1). Mitochondrial mass was measured by **(C)** MitoTracker® Green FM (ThermoFisher) staining followed by flow cytometry and **(D)** by determining the mtDNA/gDNA ratio. **(E)** A citrate synthase assay kit (Sigma-Aldrich) was applied to measured the activity of this mitochondrial enzyme. Values represent mean ± SEM of 3 mice. **P*<.05; ****P*<.001

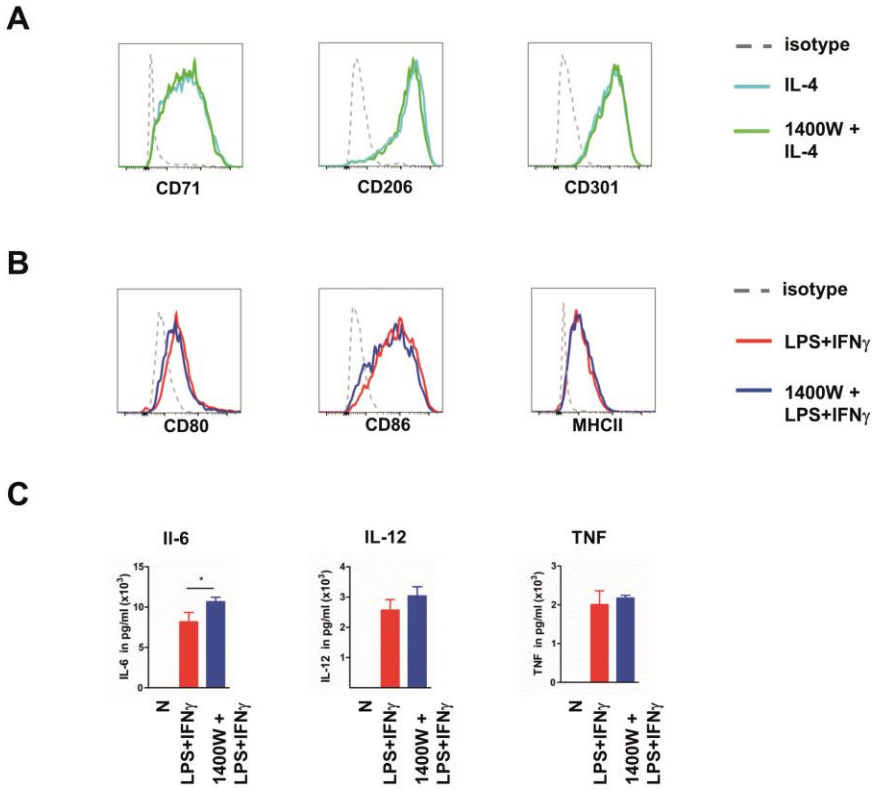

Figure S7. iNOS inhibition has no effect on M1 and M2 polarization per se. Related to Figure 6. (A) M2 polarization in the presence and absence of the iNOS inhibitor 1400W was assessed flow cytometry for CD71, CD206 and CD301 and demonstrated as histogram overlays. **(B)** M1 activation with and without iNOS inhibitor 1400W was measured by flow cytometry for CD80, CD86 and MHC-II and **(C)** by ELISA for IL-6, IL-12 and TNF. Values represent mean ± SEM of 3 mice.*P<.05.

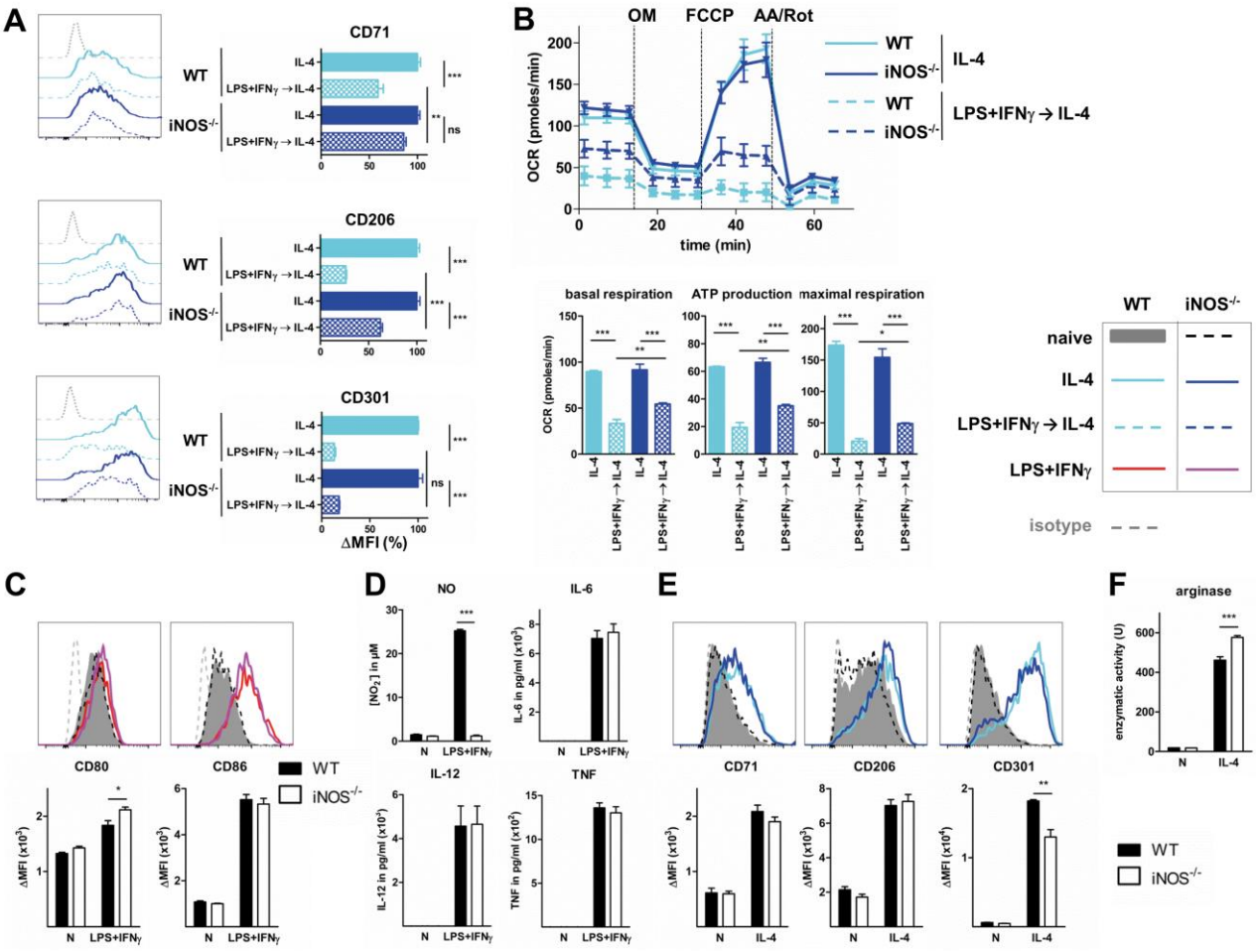

Figure S8. Nos2$^{-/-}$ show partially enhanced OXPHOS and M2 surface marker expression upon M1 to M2 repolarization. **Related to Figure 6. (A)** Phenotypic M1→M2 repolarization in WT and Nos2$^{-/-}$ BMMs was assessed by flow cytometric analysis for M2 surface markers CD71 (TFR, transferrin receptor), CD206 (MRC1, macrophage mannose receptor) and CD301 (MGL1/2, macrophage galactose-binding lectin) in comparison to the levels in IL-4-induced M2 macrophages. Representative histogram plots, together with the quantified surface expression values are shown (expression calculated as ΔMFI = [Median fluorescence intensity]$_{\text{positive staining}}$ − [Median fluorescence intensity]$_{\text{isotype staining}}$ and plotted relative to the expression in WT and iNOS$^{-/-}$ M2 macrophages (both = 100%)). **(B)** The metabolic repolarization of WT and Nos2$^{-/-}$ BMMs was measured by extracellular flux analysis. OCR values were recorded after sequential injection of OM, FCCP and rotenone (ROT) plus antimycin A (AA). Calculated basal respiration, ATP production and maximal respiration were plotted in bar graphs. **(C)** LPS+IFNγ-induced M1 polarization in WT (black bars) and Nos2$^{-/-}$ (white bars) BMMs was assessed by flow cytometry for CD80 and CD86 and **(D)** by ELISA for IL-6, IL-12 and TNF. **(E)** NO secretion was measured by Griess reaction to demonstrate knock out efficiency. **(F)** IL-4-induced M2 polarization in was assessed by flow cytometry for CD71, CD206 and CD301, and **(G)** by arginase activity assay. Values represent mean ± SEM of 3 mice.*P <.05; **P <.01; ***P <.001.

Table S1. Substrates and inhibitors for measuring complex I till IV activity, related to Figure 4.

	Complex I	Complex II	Complex III	Complex IV
	compounds (final concentration after injection)			
Port A	pyruvate(5 mM)	succinate (10 mM)	duroquinol (0.5 mM)	TMPD* (0.5 mM)
	malate (2.5 mM)	rotenone (1 µM)		ascrobate (2 mM)
	ADP (1mM)	ADP (1mM)	ADP (1mM)	ADP (1mM)
	digitonin (30 µg/ml)	digitonin (30 µg/ml)	digitonin (30 µg/ml)	digitonin (30 µg/ml)
Port B	oligomycin (15 µM)	oligomycin (15 µM)	oligomycin (15 µM)	oligomycin (15 µM)
Port C	rotenone (1 µM)	malonate (40 µM)	antimycin A (20 µM)	azide (20 mM)

* TMPD = N,N,N′,N′-Tetramethyl-p-phenylenediamine (artifical substrate to measure complex IV activity)

* all compounds were obtained from Sigma-Aldrich

* distinct complex activities were calculated as $OCR_{\text{after port A}}$ - $OCR_{\text{after port C}}$

Table S2. List of used antibodies, related to Experimental Procedures

Marker	Clone	Supplier
mouse CD16/CD32 (Fc-block)	93	eBioscience
mouse CD80/PE	16-10A1	BD Bioscience
mouse CD86/APC	GL1	eBioscience
mouse CD71/PE	C2(F2)	BD Bioscience
mouse CD206/APC	C068C2	Biolegend
mouse CD301/Alexa-Fluor-647	ER-MP23	Serotec
mouse IL-4Rα-PE	mIL4R-M1	BD Bioscience
mouse CD45.1/PE-Cy7	A20	eBioscience
mouse F4/80/APC-Cy7	BM8	eBioscience
human CD14/PE-Cy7	M5E2	BD Bioscience
human CD23/APC	EBVCS2	eBioscience
human CD200R/PE	OX-108	Biolegend
human CD206/Alexa-Fluor-488	15-2	Biolegend
human CD197/PE	G043H7	Biolegend
human CD64/APC	10.1	Biolegend
human CD86/Alexa-Fluor-488	IT2.2	Biolegend
rat IgG2a/PE or APC isotype control	R35-95	BD Bioscience
Mouse IgG1κ/FITC, PE, APC isotype control	MOPC-21	Biolegend
p-STAT6(Tyr641)	rabbit polyclonal	Cell Signaling Technology
actin	C4	Millipore
anti-rabbit IgG/HRP (secondary)	goat polyclonal	ThermoFisher
anti-mouse IgG/HRP (secondary)	goat polyclonal	ThermoFisher